RTMENT OF COMMERCE • ENVIRONMENTAL SCIENCE SERVICES ADMINISTRATION
Weather Bureau

TECHNICAL NOTE 17-NHRL-74

TECHNICAL NOTE 17-NHRL-74

A Summary of Empirical Studies of the Horizontal Motion of Small Radar Precipitation Echoes in Hurricane Donna and Other Tropical Storms

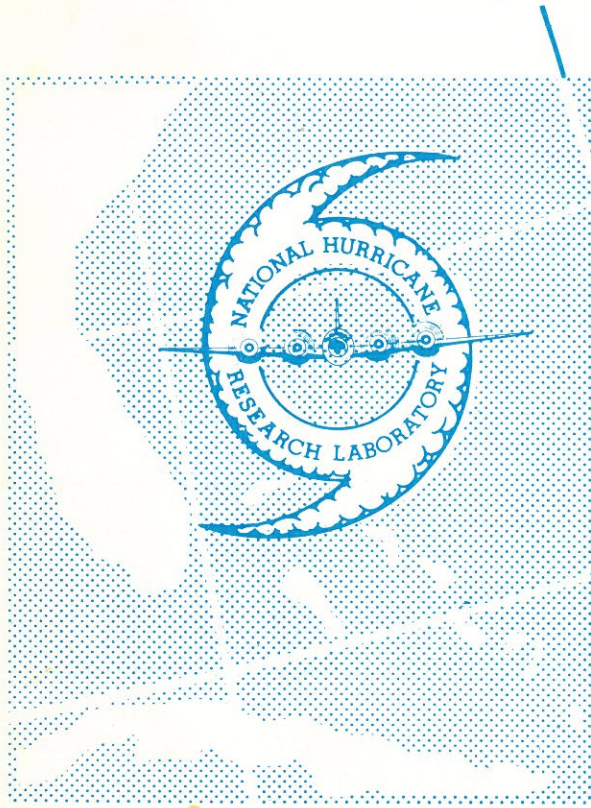

NATIONAL HURRICANE RESEARCH
LABORATORY REPORT NO.74

WASHINGTON,D.C.
November 1965

TECHNICAL NOTES SERIES

NATIONAL HURRICANE RESEARCH LABORATORY REPORTS

Reports by Weather Bureau units, contractors, and cooperators working on the hurricane problem are preprinted in this series to facilitate immediate distribution of the information among the workers and other interested units. As this limited reproduction and distribution in this form do not constitute formal scientific publication, reference to a paper in the series should identify it as a preprinted report.

The reports are available through the Clearinghouse for Federal Scientific and Technical Information, U. S. Department of Commerce, Sills Building, Port Royal Road, Springfield, Va. 22151.

No. 1. Objectives and basic design of the NHRP. Staff NHRP. March 1956.
No. 2. Numerical weather prediction of hurricane motion. L. F. Hubert. July 1956.
Supplement: Error analysis of prognostic 500-mb. maps made for numerical weather prediction of hurricane motion. March 1957.
No. 3. Rainfall associated with hurricanes. R. W. Schoner and S. Molansky. July 1956.
No. 4. Some problems involved in the study of storm surges. D. Lee Harris. December 1956.
No. 5. Survey of meteorological factors pertinent to reduction of loss of life and property in hurricane situations. March 1957.
No. 6. A mean atmosphere for the West Indies area. C. L. Jordan. May 1957.
No. 7. An index of tide gages and tide gage records for the Atlantic and Gulf coasts of the United States. D. Lee Harris and C. V. Lindsay. May 1957.
No. 8. Part I. Hurricanes and the sea surface temperature field. Part II. The exchange of energy between the sea and the atmosphere in relation to hurricane behavior. Edwin L. Fisher. June 1957.
No. 9. Seasonal variations in the frequency of North Atlantic tropical cyclones related to the general circulation. Emanuel M. Ballenzweig. July 1957.
No. 10. Estimating central pressure of tropical cyclones from aircraft data. C. L. Jordan. August 1957.
No. 11. Instrumentation of National Hurricane Research Project aircraft. D. T. Hilleary and F. E. Christensen. August 1957.
No. 12. Studies of hurricane spiral bands as observed on radar. H. V. Senn, H. W. Hiser, and R. C. Bourret. September 1957.
No. 13. Mean soundings for the hurricane eye. C. L. Jordan. September 1957.
No. 14. On the maximum intensity of hurricanes. B. I. Miller. December 1957.
No. 15. The three-dimensional wind structure around a tropical cyclone. B. I. Miller. January 1958.
No. 16. Modification of hurricanes through cloud seeding. R. R. Braham, Jr., and E. A. Neil. May 1958.
No. 17. Analysis of tropical storm Frieda 1957. A preliminary report. Herbert Riehl and R. C. Gentry. June 1958.
No. 18. The use of mean layer winds as a hurricane steering mechanism. B. I. Miller. June 1958.
No. 19. Further examination of the balance of angular momentum in the mature hurricane. R. L. Pfeffer. July 1958.
No. 20. On the energetics of the mature hurricane and other rotating wind systems. R. L. Pfeffer. July 1958.
No. 21. Formation of tropical storms related to anomalies of the long-period mean circulation. E. M. Ballenzweig. September 1958.
No. 22. On production of kinetic energy from condensation heating. H. Riehl. October 1958.
No. 23. Hurricane Audrey storm tide. D. Lee Harris. October 1958.
No. 24. Details of circulation in the high energy core of hurricane Carrie. Staff, NHRP. November 1958.
No. 25. Distribution of surface friction in hurricanes. L. F. Hubert. November 1958.
No. 26. A note on the origin of hurricane radar spiral bands and the echoes which form them. H. V. Senn and H. W. Hiser. February 1959.
No. 27. Proceedings of the Board of Review and Conference on Research Progress. Technical Conference on Hurricanes. March 1959.
No. 28. A model hurricane plan for a coastal community. Weather Bureau and Corps. of Engineers. March 1959.
No. 29. Exchange of heat, moisture, and momentum between hurricane Ella (1958) and its environment. M. Gangopadhyaya and H. Riehl. April 1959.
No. 30. Mean soundings for the Gulf of Mexico area. Paul J. Herbert and C. L. Jordan. April 1959.
No. 31. On the dynamics and energy transformations in steady-state hurricanes. J. S. Malkus and H. Riehl. August 1959.
No. 32. An interim hurricane storm surge forecasting guide. D. L. Harris. August 1959.
No. 33. Meteorological considerations pertinent to standard project hurricane, Atlantic and Gulf coasts of the United States. H. E. Graham and D. E. Nunn. November 1959.
No. 34. Filling and intensity changes in hurricanes over land. William Malkin. November 1959.
No. 35. Wind and pressure fields in the stratosphere over the West Indies region in August 1958. Hans Ulrich Groening. December 1959.
No. 36. Climatological aspects of intensity of typhoons. N. L. Frank and C. L. Jordan. February 1960.
No. 37. Unrest in the upper stratosphere over the Caribbean Sea during January 1960. H. Riehl and R. Higgs. April 1960.
No. 38. On quantitative precipitation forecasting. C. S. Gilman, K. R. Peterson, C. W. Cochrane, and S. Molansky. August 1960.
No. 39. Surface winds near the center of hurricanes (and other cyclones). H. E. Graham and G. N. Hudson. September 1960.
No. 40. On initiation of tropical depressions and convection in a conditionally unstable atmosphere. H. L. Kuo. October 1960.
No. 41. On the heat balance of the troposphere and water body of the Caribbean Sea. José A. Colón. December 1960.
No. 42. Climatology of 24-hour North Atlantic tropical cyclone movements. George W. Cry. January 1961.
No. 43. Prediction of movements and surface pressures of typhoon centers in the Far East by statistical methods. H. Arakawa. May 1961.
No. 44. Marked changes in the characteristics of the eye of intense typhoons between the deepening and filling stages. C. L. Jordan. May 1961.
No. 45. The occurrence of anomalous winds and their significance. M. A. Alaka. June 1961.

(Continued on inside back cover)

U.S. DEPARTMENT OF COMMERCE ● John T. Connor, Secretary

ENVIRONMENTAL SCIENCE SERVICES ADMINISTRATION

Robert M. White, Administrator

Weather Bureau

TECHNICAL NOTE 17-NHRL-74

A Summary of Empirical Studies of the Horizontal Motion of Small Radar Precipitation Echoes in Hurricane Donna and Other Tropical Storms

H.V.Senn and J.A.Stevens

NATIONAL HURRICANE RESEARCH LABORATORY
REPORT NO.74

WASHINGTON, D.C.
November 1965

CONTENTS

LIST OF ILLUSTRATIONS

APPENDIX - I.B.M. CARD FORMATS

LIST OF TABLES

LIST OF SYMBOLS AND DEFINITIONS

α_b crossing angle of spiral band (positive inward)

α_e crossing angle of echo (positive inward)

α_w crossing angle of wind (positive inward)

d_b width of spiral band

d_e width or diameter of echo

D_e direction toward which echo moves (rel. to storm center) CW from North

D_o original direction toward which echo moves (rel. to radar) CW from North

D_s storm direction, CW from North

k_1 parameter related to radial component of echo velocity

k_2 parameter related to tangential component of echo velocity

L_t lifetime of echo traced - number of 5-min periods

n number of observations in sample

R eye radius

r_s range of echo from storm center

r_r range of echo from radar

θ_e polar position of echo, CW from storm center velocity vector

v_e speed of echo rel. to storm center

v_o speed of echo rel. to radar

v_r radial speed of echo rel. to storm center

v_s storm speed

v_θ tangential velocity of echo rel. to storm center

Units: Angles in degrees, distances in nautical miles, speed in knots.

A SUMMARY OF EMPIRICAL STUDIES OF THE HORIZONTAL MOTION OF SMALL RADAR PRECIPITATION ECHOES IN HURRICANE DONNA AND OTHER TROPICAL STORMS

H. V. Senn and J. A. Stevens

Radar Meteorological Section, Institute of Marine Science,
University of Miami

ABSTRACT

Echo vectors relative to the storm center, obtained by vectorially subtracting storm center motion, are analyzed for 3805 traced echoes from hurricane Donna radar film. Distributions of crossing angle and radial and tangential echo motion components are presented for various storm speeds, quadrants, and ranges from the storm center. Detailed studies show that significant differences in echo motion exist between the echoes which are observed over land and over water, and also between those observed during the nighttime and daytime periods. The dependence of echo speed on crossing angle was obtained. When the dependence of echo motion on height was studied using height as a function of range from radar, results were inconclusive. However, comparisons of echo and wind kinematics produced significant relationships which varied from quadrant to quadrant. It is also found that outward moving echoes have higher speeds than inward moving echoes in the front quadrants (the opposite being the case in the rear quadrants); that echo speeds increase with increasing storm speed; and that the absolute crossing angles of the echoes decrease with increasing storm speed. Echo lifetime studies showed that the longest lived echoes are found in the left quadrants; the mean lifetime was found to be 35 minutes, and echo lifetime is related to echo diameter.

When the Donna echo motion data are compared to three sets of other echo data consisting of about 2200 echoes from nine other storms, it is shown that similarities exist between the various sets of data, including the relations between right and left quadrants in both speeds and crossing angles of echoes. In addition, data from hurricane Carla are used to show differences in echo motion due to echo environment with respect to spiral bands. Possible reasons for some of the observed echo motion characteristics are discussed.

1. INTRODUCTION

Radar Hurricane Data

Despite the fact that radar has been in use for a number of years in tracking hurricanes, advances in its usefulness as an operational tool to provide more sophisticated information about such storms have been slow. Within certain limits, it is possible to gain quantitative knowledge of the precipitation distribution around the hurricane from proper radar data; but the motion of such elements and their relation to other meteorological parameters (knowledge of which would be powerful and useful operational and research tools) have probably not received sufficient attention.

The major difficulty in radar hurricane research has always been the lack of really good radar data which encompassed a significantly large part of the life history of a particular storm. This particular difficulty was partly overcome in the case of hurricane Donna, September 9 and 10, 1960. Hurricane Donna was a major hurricane and the first hurricane to be under surveillance of many land-based radars simultaneously. The storm approached the Florida Keys on September 9, passed up the Florida southwest coast and crossed over the coast just north of Ft. Myers on September 10 (see fig. 1). During this period the storm was under continuous radar surveillance, both while it was over water and while it was over land, and during both day and night hours. Fortunately, several of the many radars observing the storm obtained filmed radarscope data of exceptionally good quality, thus making possible the first completely detailed study of radar echo motion in a single hurricane. Certain reservations have been made regarding the accuracy of some radar data for hurricane tracking and quantitative preciptitation studies [6], [3]; but these reservations do not apply to the results presented here, since all individual echoes are relative to only a single radar. While echo placement accuracies with respect to a given radar are only of the order of several degrees azimuth or several miles, the relative positions of echoes with respect to others appearing on the same radarscope or with respect to the storm center are much more precise.

The increased use of hurricane radar data in both operations and research can not be effective unless the storms are described, as well as merely observed. Only after adequate descriptions are available can we begin to explain the processes which give rise to the observed results. Consequently, empirical studies of the motion of small radar precipitation echoes have been undertaken for several years at the University of Miami, as data have become available. Good time lapse data on vertical echo motion are still relatively scarce. This project has therefore been concerned primarily with horizontal motions, including, where possible, the differences in horizontal motion which may exist in different layers.

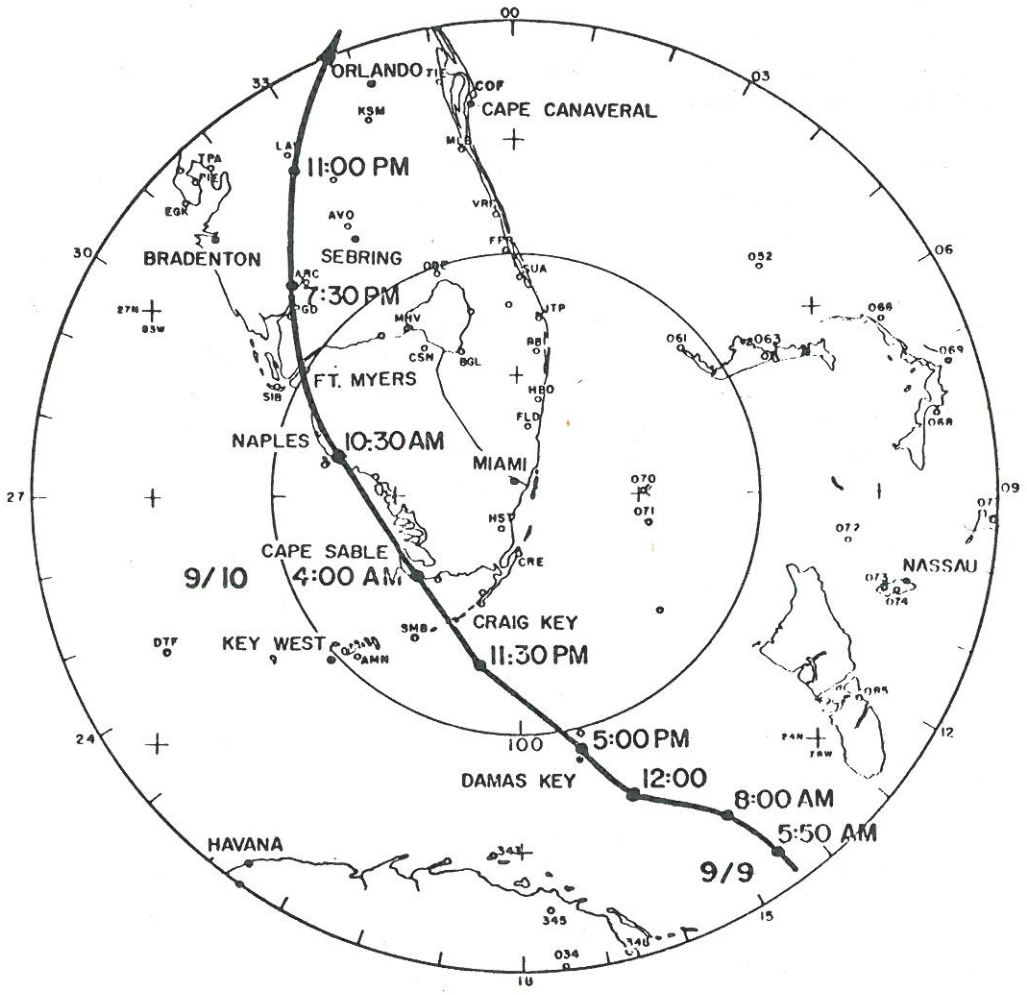

Figure 1. - Track of hurricane Donna, September 9-10, 1960.

Studies Performed

This paper presents the results of a number of preliminary studies to determine for the first time the complete picture of the simultaneous horizontal echo motion at all ranges and azimuths from the storm center. The advantages and superior results obtained from the Donna data over those of previous studies [7] which, of necessity, combined data from various ranges and azimuths of many hurricanes at different latitudes, observed by different radars from various positions with respect to the storm center, were obvious in terms of greater refinement, both of data and results. The greatest part of this summary will therefore be devoted to the more complete and representative Donna studies.

These studies were concerned with a number of very basic questions whose answers should provide significant progress in hurricane radar research as well as suggest additional operational applications:

(1) What is the statistical distribution of echoes, their speeds (tangential and radial), and crossing angles with respect to range and azimuth from the hurricane center?

(2) Are there relationships between the above distributions and the (large or small scale) motion of the storm center?

(3) Are there measurable effects on echo parameters when there are changes in the external environment (i.e., day/night, land/water) of the hurricane system?

(4) Can normal PPI scanning radars detect variations in echo motion with height?

(5) What is the specific dependence of echo speed on crossing angle?

(6) What is the relationship between the radar echoes and the winds observed at various levels in the hurricane?

(7) What is the average echo lifetime inside and outside spiral bands; and is the lifetime of an echo directly related to its diameter?

The results of the Donna studies were compared, where possible, with the results of previous studies [7], [13], [12], and with the results of the more recent Carla studies, which appear here for the first time.

It is apparent that it is not yet possible to answer fully some of these questions because of lack of data which directly applies to the problem, questions 4 and 6, for instance. In fact, attempts to answer important questions such as these, or ones relating to changes in hurricane radar parameters with time over water, have all been relatively inconclusive because of the lack of well documented, continuous, exactly comparable, quantitative radar data.

While the airborne radar might seem well suited to the gathering of such data, in the past such radars have rarely been well calibrated or the film well documented; their characteristics, and the environments and heights at which they operate, make them, more often than not, unsuited for the job. Continuous and exactly comparable data are rarely possible because of the rapidly moving platform, the varying mission requirements (most of which may take precedence over the gathering of radar data), and the relatively short mission endurance of a single aircraft in a storm. Furthermore, there are great difficulties in using time lapse data obtained from a platform whose motion characteristics, with respect to the moving storm elements, are difficult to ascertain, even for the better data. A

far better, and often hopefully suggested, solution would seem to be the maintenance of one or two ships in positions fixed with respect to the moving storm center. They might remain reasonably close to the storm center in areas of less than gale force winds, carry radars better suited to the gathering of meteorological data, use a GPI (ground position indicator) on which a fixed point - the hurricane center - would remain in the center of the radarscope, and have sufficient endurance to ensure continuous surveillance. Most of the difficulties associated with the airborne platform in obtaining radarscope data would thus be overcome. If the area of the storm were chosen carefully - left rear quadrant, for instance - a submarine might even be used with relative ease. The purpose would not be to replace many aircraft in tracking the storm in the wide oceanic areas, but to provide much more accurate and continuous data for operational and research uses at low levels.

2. DATA FORMAT

Data Used

The specific radar data used in the Donna studies is shown in table 1 which indicates the number of echoes used from the filmed radarscope data of the University of Miami 4.6-cm. MPS-4 and 10.7-cm. SP-1M radars, the U. S. Weather Bureau 10-cm. WSR-57 at Miami, and the U. S. Air Force 23-cm. FPS-20 at MacDill Air Force Base near Tampa. See [6] for characteristics of these radars.

Previously, data from seven different storms (the "seven storms data" from Edna 1954, Connie, Diane, and Ione 1955, Audrey 1957, and Daisy and Helene 1958) were obtained largely from different radars. Their characteristics can be found in [7] and the data used appears in table 2. Subsequently, data from hurricane Debra taken on the Texas A and M CPS-9 radar were used to examine echo motion, see table 3. The U. S. Weather Bureau WSR-57 radar at Galveston, Tex. supplied the data, in table 3, which was used in the more recent Carla echo studies.

TABLE 1. - HURRICANE DONNA ECHO DATA USED

Year	Radar	Begin	End	Total No. Echoes
1960	MIAC. WSR-57	1010E-9/9	1605E-9/10	1004
1960	MACDILL FPS-20	0720E-9/9	0005E-9/10	1456
1960	U.M. MPS-4	1550E-9/10	1820E-9/10	109
1960	U.M. SP-1M	0645E-9/9	1135E-9/10	1236
				3805 Total

TABLE 2 - SEVEN STORMS ECHO DATA USED

Storm	Year	Radar	Begin	End	Total No. Echoes
Edna	1954	M.I.T.	0000E-9/11	1145E-9/11	258
Connie	1955	HAT. SP-1M	0040E-8/11	0520E-8/12	22
Diane	1955	HAT. SP-1M	1400E-8/16	2045E-8/17	96
Ione	1955	HAT. SP-1M	1146E-9/18	0940E-9/19	150
Ione	1955	S. TRURO FPS-3	0100E-9/20	1940E-9/20	73
Audrey	1957	ELL. A.F.B. CPS-6B	0600C-6/27	2030C-6/27	85
Audrey	1957	ALEX. A.F.B. A.D.C.	0025C-6/28	0055C-6/29	196
Daisy	1958	HAT. SP-1M	0726E-8/28	1647E-8/28	126
Daisy	1958	NKT. SP-1M	1320-8/28	1212E-8/29	59
Daisy	1958	U.M. MPS-4	1202E-8/26	1505E-8/27	115
Daisy	1958	PAT CPS-9	0124E-8/27	1950E-8/27	78
Helene	1958	HAT. SP-1M	0035E-9/27	1935E-9/27	202
Helene	1958	CHS. WSR-1	0000E-9/26	0940E-9/27	107
					1567 Total

TABLE 3. - DATA USED FROM HURRICANES DEBRA AND CARLA

Storm	Year	Radar	Begin	End	Total No. Echoes
Debra	1959	TEXAS A and M CPS-9	1700C-7/24	2115C-7/24	600 (Approx.)
Carla	1961	GLS. WRS-57	1225C-9/10	1636C-9/10	67

Data Reduction

Figure 2 shows the relationship between the various storm center, echo, and spiral band parameters used in analyzing the Donna data. Crossing angle, "α_e" is defined as the angle between a secant line and the tangent to a circle passing through the point in question and having the hurricane center as its center. The angle α_e was obtained, with other parameters, from the best straight line vector approximation of 5 min. tracings of relatively isolated small, hard-core echoes.

In most cases, the tracing was done with the aid of a Nemeth Radar Data Plotter with the 35-mm. film image magnified about 50 times. When possible, the storm center was fixed to a given point on the tracing before the echo or spiral band position was recorded resulting in echo motion relative to the

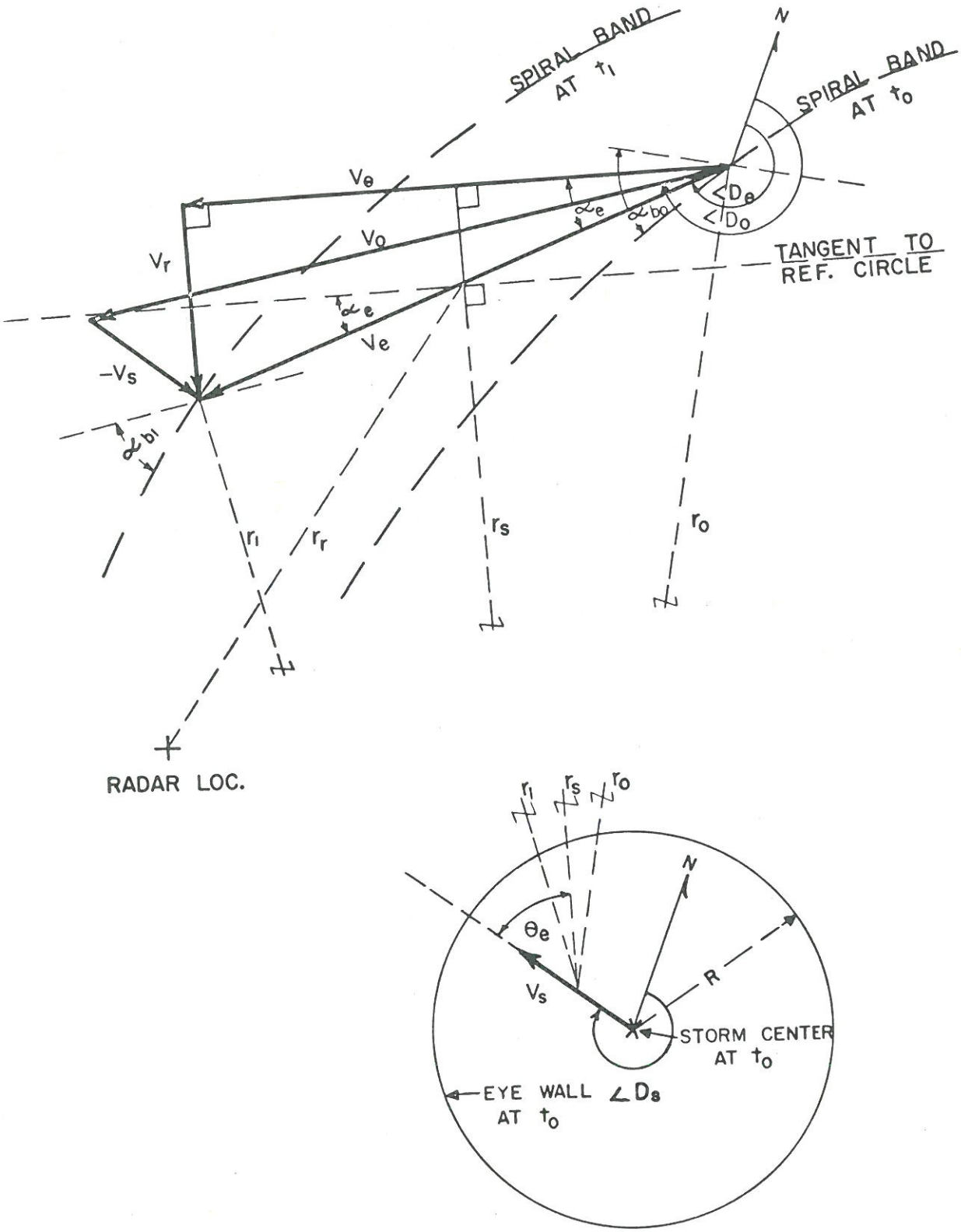

Figure 2 - Relationships between various spiral band, echo, and storm center parameters. Refer to list of symbols for definitions of variables.

storm center (as contrasted to motion relative to a fixed point on the earth, the radar station, which was obtained when no clear cut storm center was available on the same photograph).

The crossing angle of each echo, its range and azimuth from the storm center, etc., were all measured with respect to a line through the center of the echo vector and the center of the storm motion vector for the same time period. This is shown in figure 2 which illustrates the variables recorded. In addition, original echo data which used actual simultaneous small-scale eye motion were recomputed using a 30-min. running mean storm center velocity. Both sets of echo and storm speed values appear on the IBM cards, enabling the comparison of three types of echo motion: the relative echo motion obtained by use of short-period, simultaneous storm motion data; the relative motion obtained with a longer-period average storm motion; and the actual motion relative to a fixed point on the earth - the radar site.

The echoes used in the hurricane Donna and previous studies were assumed to lie within the confines of spiral bands. While this might be a valid assumption from the standpoint that the major precipitation areas consist of such banded echo areas, individual small echoes are easier to find and analyze outside of the bands. Since the bands are not well defined, a decision must be made for each echo as to whether it is within or outside a band. This decision might also require modification with time as a given echo moves into a different environment. Such analysis was too time consuming for each echo and therefore was not performed when the sample included thousands of echoes. However, a separate study was subsequently made on Carla echo data to determine such effects. The Carla data presented later were obtained even more precisely than those for previous studies; but they are somewhat limited in scope and results must be considered preliminary.

Reproducibility of Data

Extensive studies were made to determine whether echo velocity data could be reliably reproduced by an independent analyst. Studies of several hundred echoes from three different radars showed that echo crossing angles were generally reproduced within $\pm 4°$ when the entire process was duplicated. When only the reduction of existing velocity vectors from a tracing was duplicated, the differences between independent analysts were less than $\pm 2°$ for 85 percent of the duplicated echoes. For one large group of echoes, the analysts agreed exactly on crossing angle for 30 percent of the echoes. Reproducibility of the data was therefore considered to be excellent and well within the limits of accuracy necessary for an extensive statistical treatment of the echo data.

Card Format

All of the data taken in hurricane Donna were reduced to a set of IBM cards, one echo per card. The arrangement of the pertinent data for each echo on the card is shown in figure A1 in the Appendix. Definitions of most of the basic variables are given in the List of Symbols at the beginning of the report.

There were, of course, a number of intermediate computational decks, which were described in [12]; but the master deck shown in figure A1 is the one available for computation using the 3805 card deck of Donna data, and contains all pertinent quantities that are presently available from either direct measurement on the radarscope film or through computations for individual echoes.

The card plan used for the seven storms data is shown in figure A2 in the Appendix. These data were obtained in a slightly different manner from the Donna data (different projection equipment, different storm center track, some variables not registered), and are considered neither as accurate nor as useful as the Donna data. However, the deck has been used for IBM machine calculations of the relationship between precipitation element variables as reported by Senn, et al., in [9], [10].

The Debra data were not obtained on the same plan as other studies. Some of the variables were omitted and the data were not placed on cards but were computed by hand for special investigation. Although a much more sophisticated plan is being used presently for the compilation of data from Carla, it has not yet been necessary to place that information on cards for machine handling.

This plan is shown in the Appendix as figure A4.

Techniques of Analysis

The Donna data used in these studies were analyzed using computer techniques on large statistical samples of echoes. The following illustrates the step-by-step computer computations performed in the reduction of the data.

(1) About one-third of the echo data used were obtained from film on which storm center did not appear. The radar site was used as the reference point. Since echo motion relative to the storm center was required, it was necessary to compute this motion using storm motion obtained from another source. The remainder of the data had been originally obtained relative to instantaneous storm motion plotted at 5-min. intervals coincident with the echo motion. To make the data fully compatible, the echo motion had to be recomputed relative to a uniform average storm speed, shown as a function of time in figure 3. This figure is a 1/2 hour running mean derived from a 5-min. plot of storm speed. The importance of the regular oscillations that show up in the storm speed has been discussed by Senn [12], who also demonstrated the reproducibility of this phenomena when other radars are taken into account. Figure 3 is a composite from all the radars that viewed

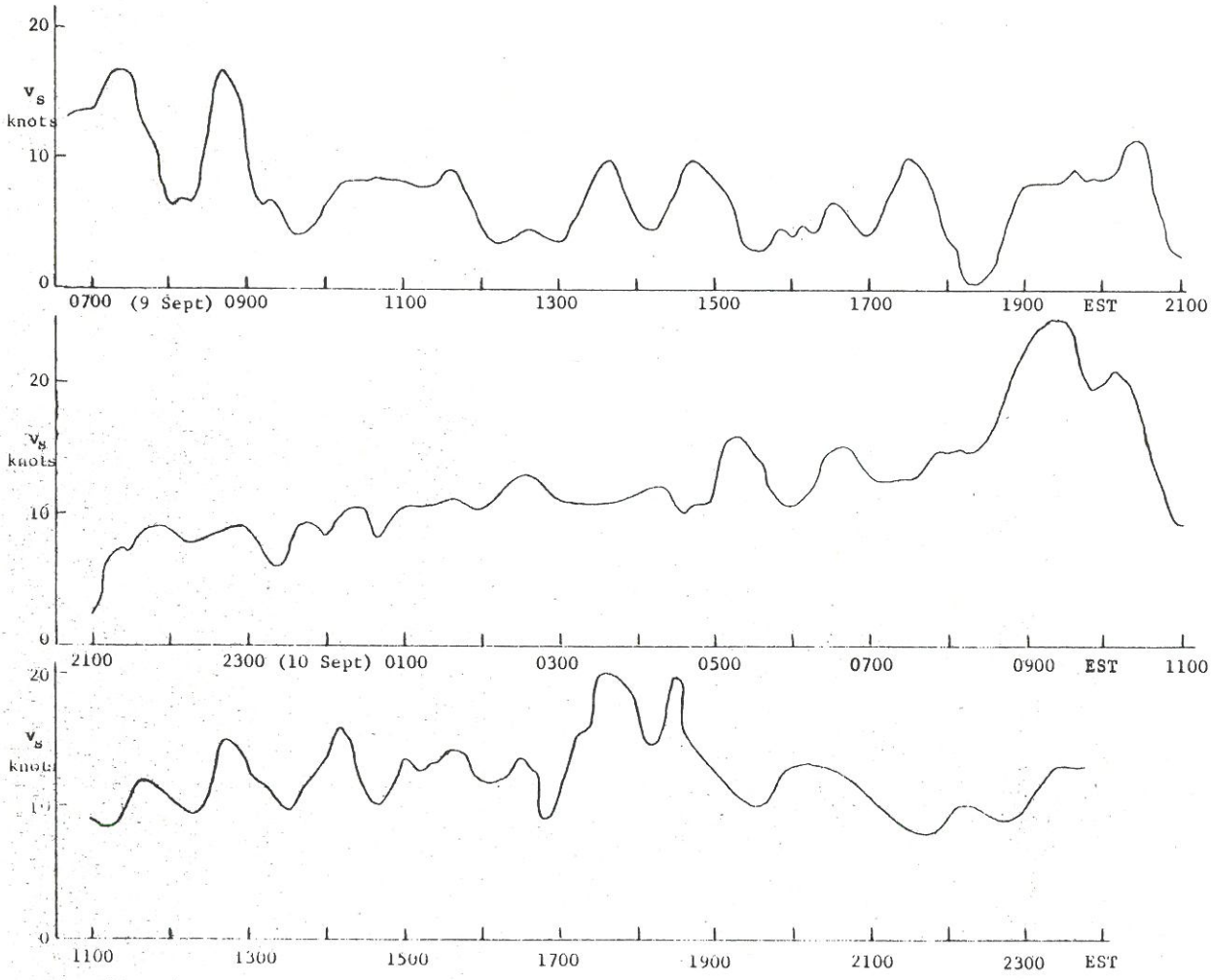

Figure 3. - Hurricane Donna storm speed, September 9-10, 1960.

the storm, the overlapping portions of which agree with one another. It was also desired to resolve the echo motion into tangential and radial components at the same time. These three separate steps were accomplished by a program for the IBM 1620 entitled DONNA I.

(2) The second phase of the computational program was to obtain distributions of all variables with range, azimuth, and storm speed. This program, the results of which appear in section 3, was entitled DONNA II. The output was a print-out of the averages of the pertinent variables n, v_e, $\bar{v}_e$, and v_r broken into classifications of quadrant, 20 n. mi. range increment, sign of crossing angle, and magnitude of storm speed.

(3) The third phase of computation, using a program called DONNA IV, was designed to produce a more detailed echo distribution with azimuth (30-deg. sections), a distribution of echoes with storm speed, and a

distribution of signed crossing angles with storm speed. These results also appear in section 3.

(4) The fourth phase of the program was to repeat part 2 above with the objective of determining environmental differences in the results. For this purpose the data were broken down with respect to day-night and land-water. These results are shown in section 3.

(5) Finally, part 2 was repeated again in an attempt to determine whether differences occurred in the motion as a result of the different heights of echoes. For this purpose the data were broken down with regard to range from radar as the parameter which gives some indication of the height of the echo. The results are presented in section 3.

3. ANALYSIS

Distribution of Echoes and Dependence of Echo Parameters on Storm Speed

The distributions of echoes here presented are intended to completely define the locations of echoes; under the conditions of echo selection such distributions do not necessarily have absolute physical significance. Figure 4 is here presented for the purpose of indicating the relationship between the radarscope presentation and the echo-selection process. It can be seen from figure 4 that the traceable echoes are found mostly on the outer fringes of spiral bands, and in the tails.

It must be emphasized that all the graphs pertaining to this section represent predominantly small, hard-core, easily trackable echoes and not the real distribution of echoes in the storm. Clearly, the density of echoes in spiral bands and in the wall cloud is so high that there are few representatives in the collected data.

These studies show that while echoes generally are advected by the wind layers in which they are embedded, important differences are present between echo motion and winds. The reader is therefore cautioned against assuming an exactly linear relationship between winds and echo motion characteristics as the latter are presented throughout this report.

In order to study some of the echo characteristics which were masked by the time averaging processes used in the seven storms, Debra, and Donna studies, echoes were traced from hurricane Carla data. In this study the aim was not to obtain a large statistical sample but to have all echoes in one sample obtained simultaneously, and then to study variations in the distribution due to position with respect to radar storm center, spiral bands, etc., as for the earlier data. However, it is apparent even for the Carla data that the echoes were selected carefully for other characteristics (i.e., convenience of tracing, size, intensity, etc.) and therefore are not representative of the actual distribution of echoes in the storm at any particular time.

The over-all distribution of the trackable radar echoes throughout Donna shown in figure 5 was obtained by plotting the actual number of

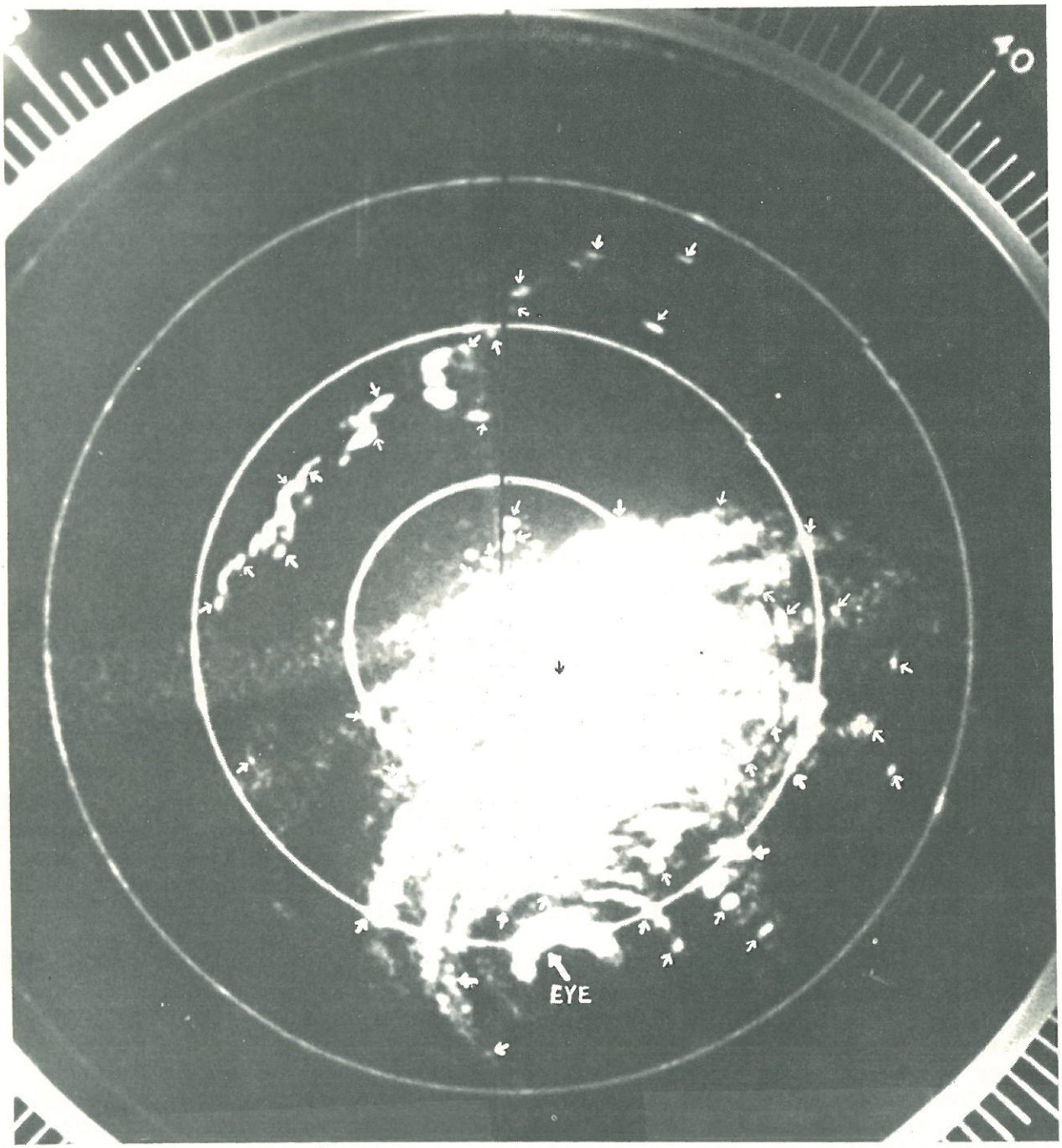

Figure 4. - Example of echoes used for motion studies. Donna, 1645 EST, September 9, 1960, University of Miami SP-1M radar, antenna tilt +0.05, 5μsec. pulse, 50 n. mi. range circles. (Some echo definition which is clearly apparent in the original time lapse film is unavoidably lost in reproduction.)

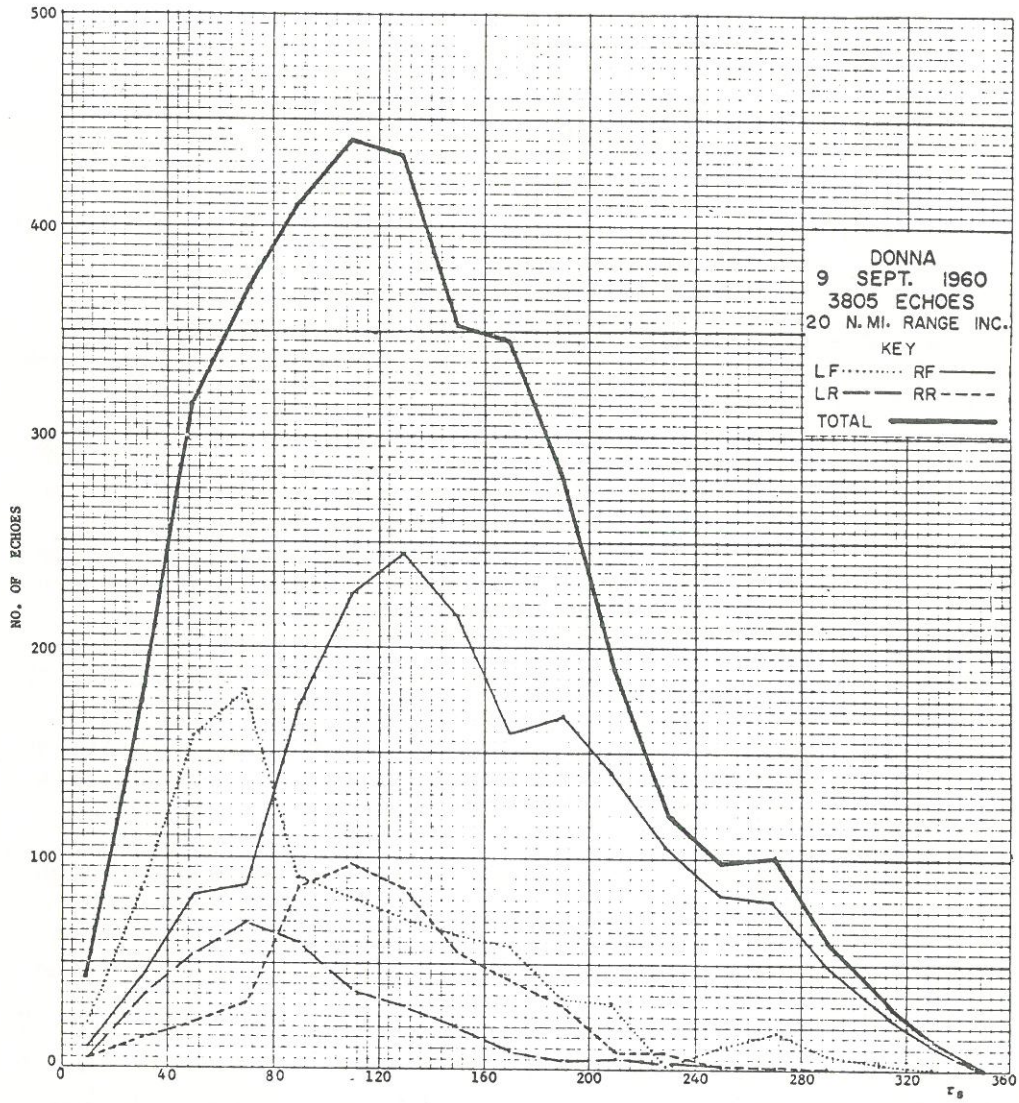

Figure 5. - Distribution of echoes vs. range for each quadrant.

observed echoes vs. range from storm center for all echoes and for each quadrant separately. Although no attempt was made to trace all of the relatively small and well defined echoes, the great number of trackings suggests that figure 5 should be representative of the general distribution of such echoes in Donna. It is apparent that the great majority of echoes were found between the ranges of 40 and 200 n. mi. from the storm center. It is often difficult to find well defined small echoes in the vicinity of the eye wall, so relatively few echoes were traced in this region. However, several non-hurricane factors contributed to the relatively large number of echoes at greater ranges out to and beyond 300 n. mi.: the position of three out of four of the radars in the right front quadrant of the hurricane for a very long period from the time the storm was several hundred miles away until it had passed to the south and west, recurving around the radars; the fact

that several of the radars discontinued operations relatively few hours after the storm's passage, having used most capabilities many hours prior to its passage; and the absence of cameras on upstate Florida radars otherwise capable of documenting accurate eye motion, resulting in loss of much of the later data.

Figure 5 indicates that most of the suitable echoes were found in the right front quadrant, with a maximum at 130 n. mi. and the great majority of all echoes found beyond about 100 n. mi. from the storm center. While this is due partly to radar factors listed above, this is also typical of the echo distribution in well defined hurricanes which are moving at average rates for the region between 15° and 35° N. latitude.

The relative number of echoes found in the other three quadrants also seems representative at most ranges. The data for the right rear quadrant probably suffered most at long ranges from the radar factors enumerated above. Much of the unused echo data on hand were drawn from great ranges in the right rear quadrant, which were not included in this study because no accurate concurrent radar storm center motion was available.

An important feature of figure 5 is the range of the maximum number of echoes observed in each quadrant. Since the right quadrants were well covered by three of the four radars, the peaks are probably representative. However, with the storm at least 60 n. mi. to the west of the same radars (storm heading nearly north), the range beyond 100 n. mi. in the left quadrants received little or no coverage. Lesser ranges in the left quadrants could not be adequately covered because of the increasing height of the radar beams with distance and loss of echoes from partial or complete "overshooting." The 70-n. mi. peaks in the left quadrants may therefore be too near to the storm center, the real peaks being somewhat closer to the right quadrant peaks, but not necessarily as far out.

Figure 6 shows the distribution of all the echoes with azimuth in hurricane Donna. In this as in other references to echo azimuths in this study, the angles are measured clockwise from the direction of storm motion. For angles measured in this way, the right front quadrant is the angular segment 0°-90°, the right rear 90°-180°, the left rear 180°-270°, and the left front 270°-360°. Nearly half of the echoes meeting selection criteria are found in the right front quadrant, with very few echoes found in the left rear quadrant. This is to be expected since the mechanism that generates echoes appears to proceed with its greatest vigor in the right front quadrant, with secondary vigor in the adjacent quadrants, and with its least vigor in the left rear quadrant. Despite the fact that data were obtained from four radars, this curve shows that the sample is apparently representative with respect to azimuth.

Figure 6 also shows the distribution around the storm of fractions of echoes possessing signed crossing angles at all ranges in a given azimuth. Over 50 percent of the echoes between the azimuths of 330° and 180° (i.e., mainly in the right quadrants) possess inward crossing angles, while about 30 percent possess outward crossing angles and 10-20 percent possess zero crossing angles at those azimuths. The boundary between the right rear and left rear quadrants shows the greatest fraction of zero crossing angles, while the boundary between the left rear and left front quadrants is the region having the largest fraction of outward crossing angles. Inward crossing angles predominate by a wide margin in all quadrants except for about 100° of azimuth from 220° to 320°.

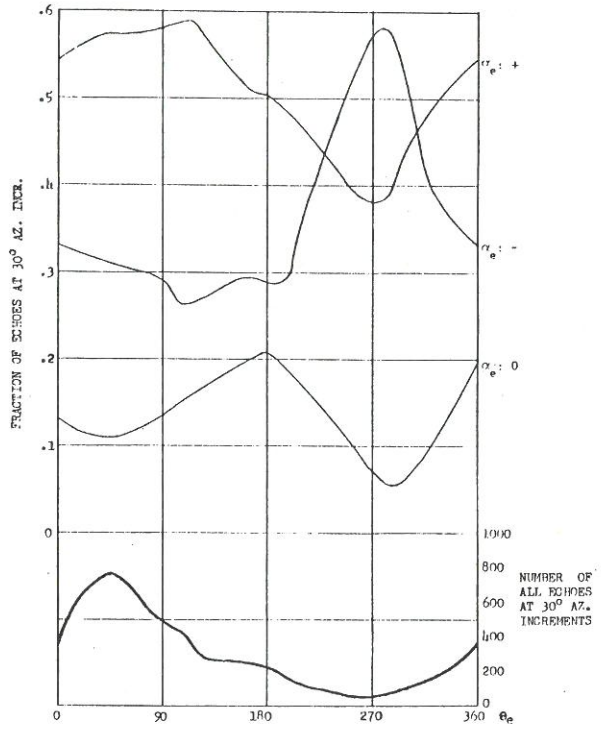

Figure 6. - Distribution of all echoes and fractions of echoes with signed crossing angles vs. azimuth in hurricane Donna.

A significant point in the comparisons of figures 5 and 6 is that the azimuth with the greatest fraction of outward moving echoes contains the smallest number of total echoes. Also, the greatest fraction of inward moving echoes occurs in the region which has the largest number of echoes.

Figure 7 represents the distribution of number of echoes vs. echo speed for low (less than 9 kt.), medium (9-12 kt.) and high (greater than 12 kt.) storm speeds, plotted at 10-kt. increments of echo speed in Donna. For various storm speeds there is very little difference in the average echo speed observed, since the curve maxima or modes all fall between 33 and 37 kt. While the distributions for low and medium storm speed are symmetrical, that for high storm speed exhibits two pronounced secondary maxima.

The number of echoes found in the entire storm in each 2-kt. increment of storm speed is plotted in figure 8 together with the fraction of this total found in each of the four quadrants. It is clear that the frequency with which Donna moved in a given speed interval determines the size of the echo sample in that interval. It may be observed that the vast majority of the echoes were found at the medium storm speeds, with far fewer echoes obtained for low and high storm speeds. The choice of the limits of v_s medium places the oscillating storm speed in this category more often than in either the low or high storm speed classifications, as can be seen in figure 8.

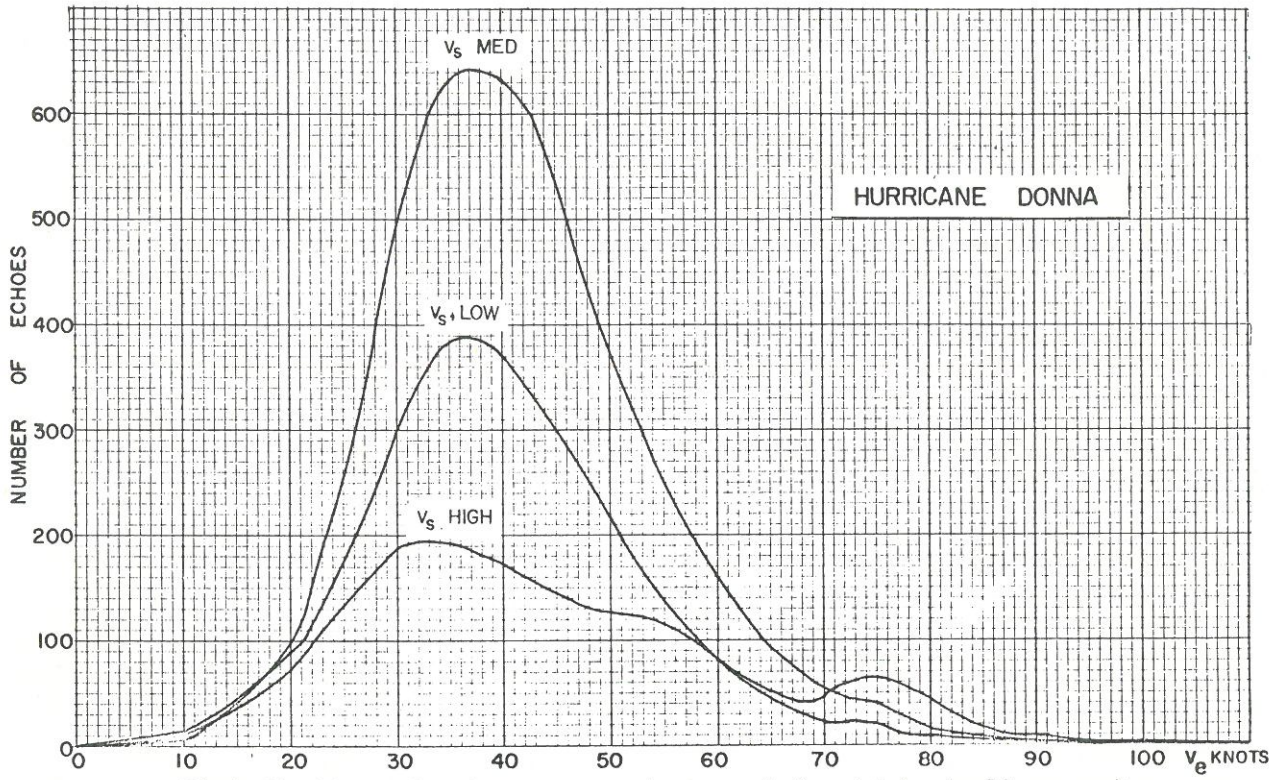

Figure 7. - Distribution of echoes vs. echo speed for high, medium, and low storm speeds; plotted in 20 n. mi. increments.

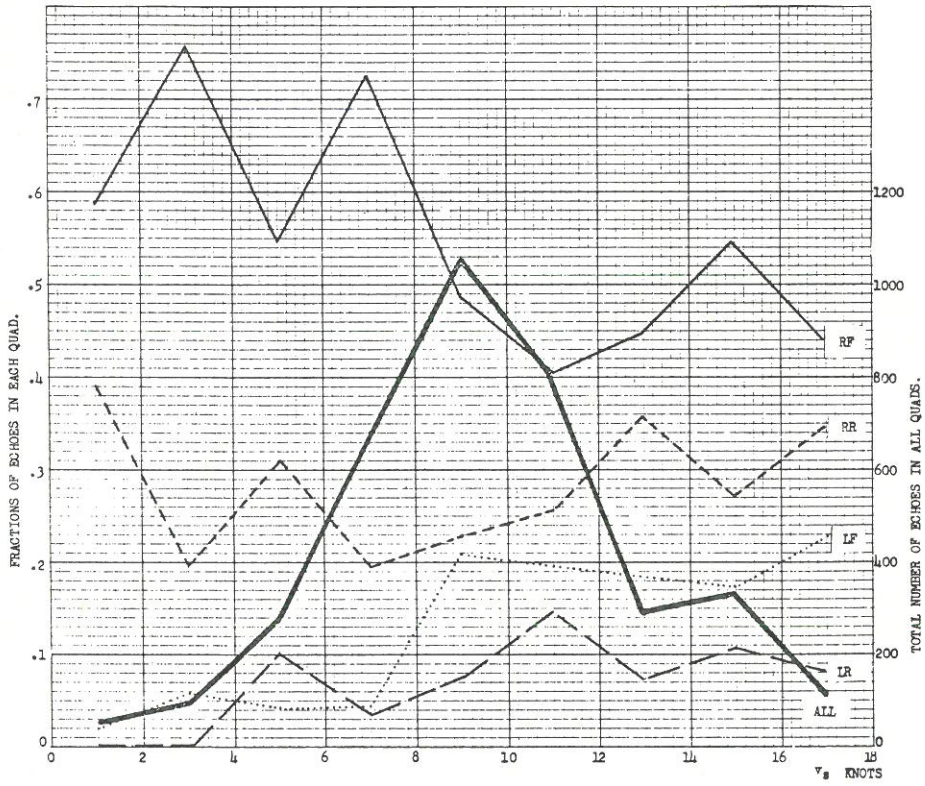

Figure 8. - Distribution of all echoes and fractions appearing in each quadrant vs. storm speed in Donna, 2 kt. increments.

For all storm speeds more echoes were found in the right front quadrant than were found in all the others; more were found in the right rear quadrant than in the left quadrants; and more were found in the left front quadrant than in the left rear, except for storm speeds between 4 and 7 kt. All plots of combined-quadrants data against storm speed, then, are biased toward the right front quadrant in preference to the others, and also biased in favor of the right semicircle. To avoid such bias and to exhibit true relationships between the variables, most data have been plotted by individual quadrants and for high, medium, and low storm speeds separately, in the graphs which follow.

Figure 9 shows echo speed (v_e) vs. storm speed (v_s) for signed echo crossing angles in each quadrant. These graphs show: (a) that the slowest echoes are in the front quadrants (for most values of α_e) at all but the low v_s, and the fastest echoes are in the front quadrant at low v_s, and the left rear quadrant for all v_s and α_e; and (b) that v_e rises with increasing v_s (beyond about v_s = 7 kt.) in all cases except in the left front quadrant for zero and positive α_e.

Figure 10 shows α_e vs. v_s in each quadrant. In general, it is shown that inward moving echoes have crossing angles which decrease in magnitude as the storm speed increases (except for medium and high storm speeds in the left front quadrant). At storm speeds greater than about 6 kt., outward moving echoes have markedly constant crossing angles in all quadrants (except the left front, where crossing angles decrease with increasing storm speeds). For most storm speeds above 8 kt., the largest outward crossing angles are found in the left rear quadrant, and the smallest in the right rear quadrant; while the largest inward crossing angles are found in the right front quadrant, with the smallest found in the left front quadrant. Although the graphs are weighted means of α_e at each v_s, some values of v_s may represent very few samples so that only the gross features can be considered reliable.

Radial Dependence of Parameters

The speed of the echoes in Donna relative to the storm center is plotted against range for signed crossing angles at high and low storm speed in each quadrant in figure 11. It can be seen that for nearly all ranges, inward moving echoes have higher speeds than outward moving echoes for three cases: at high storm speeds in the left quadrants, and at low storm speeds in the right front quadrant. In the other cases outward moving echoes move faster than inward moving echoes. Except for the left front quadrant, there is a much larger variation of echo speed with range at high storm speeds than there is at low storm speeds (from 40 kt. peak to minimum in the left rear quadrant for outward moving echoes, to 15 kt. peak to minimum for inward moving echoes in the left rear quadrant). For ranges greater than 150 n. mi. the echo speeds are generally less at high storm speeds than at low storm speeds, except for inward moving echoes in the left rear quadrant. An increasing dependence of echo speed on storm speed is thus demonstrated for ranges less than 150 n. mi.

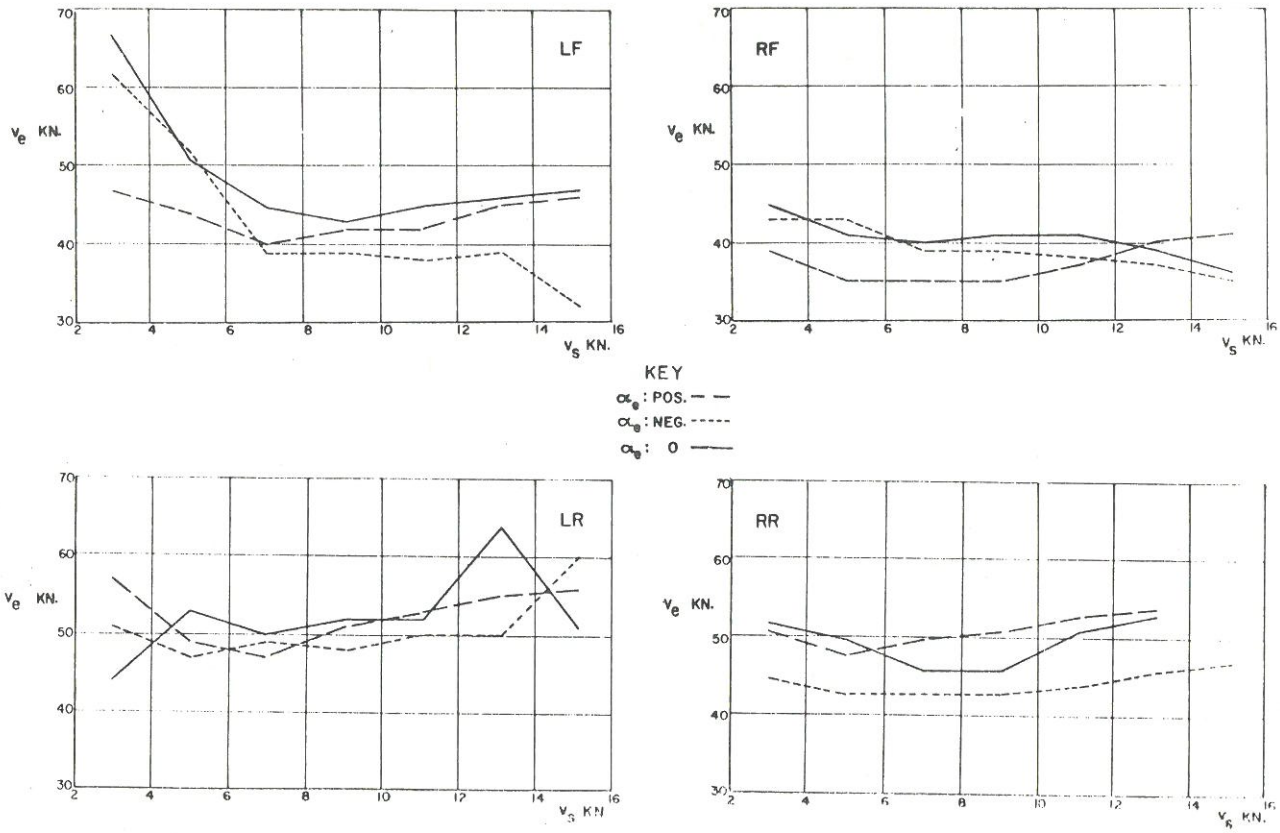

Figure 9. - Echo speed vs. storm speed for signed crossing angles in each quadrant.

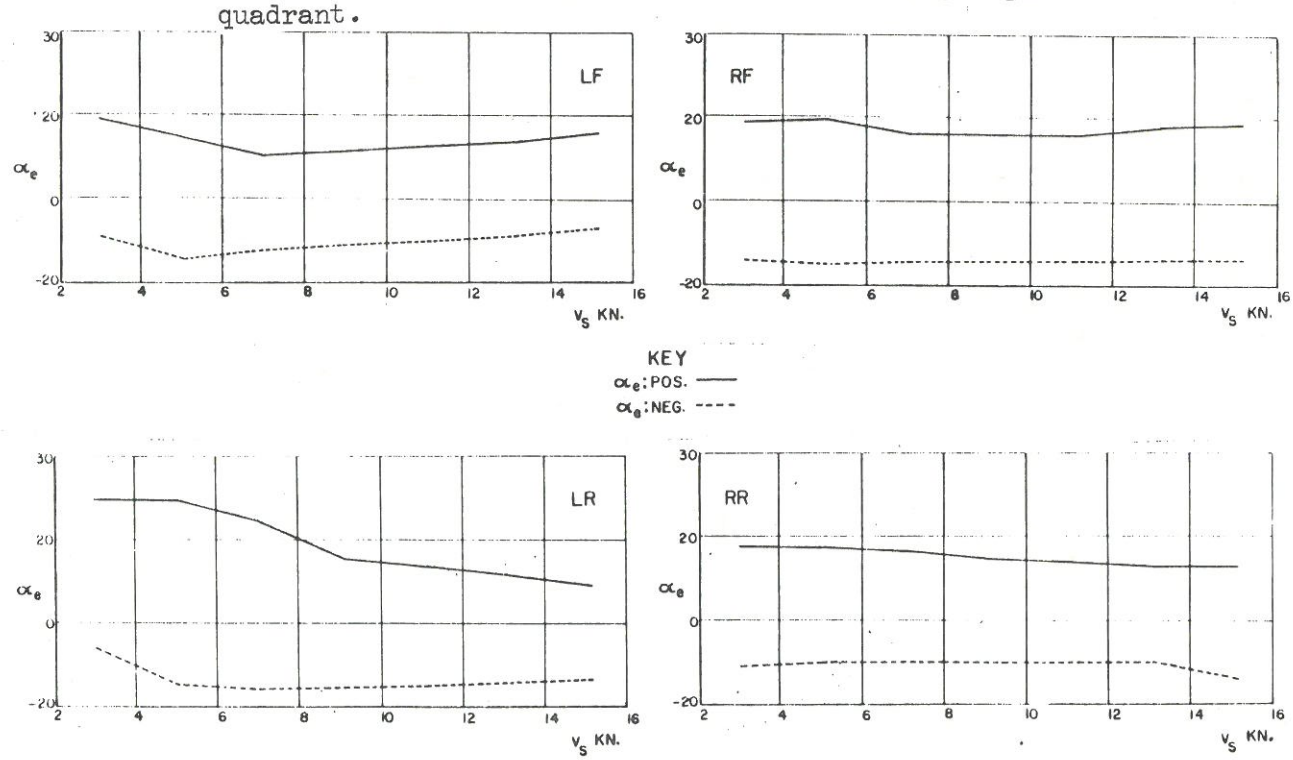

Figure 10. - Echo crossing angle us. storm speed in each quadrant.

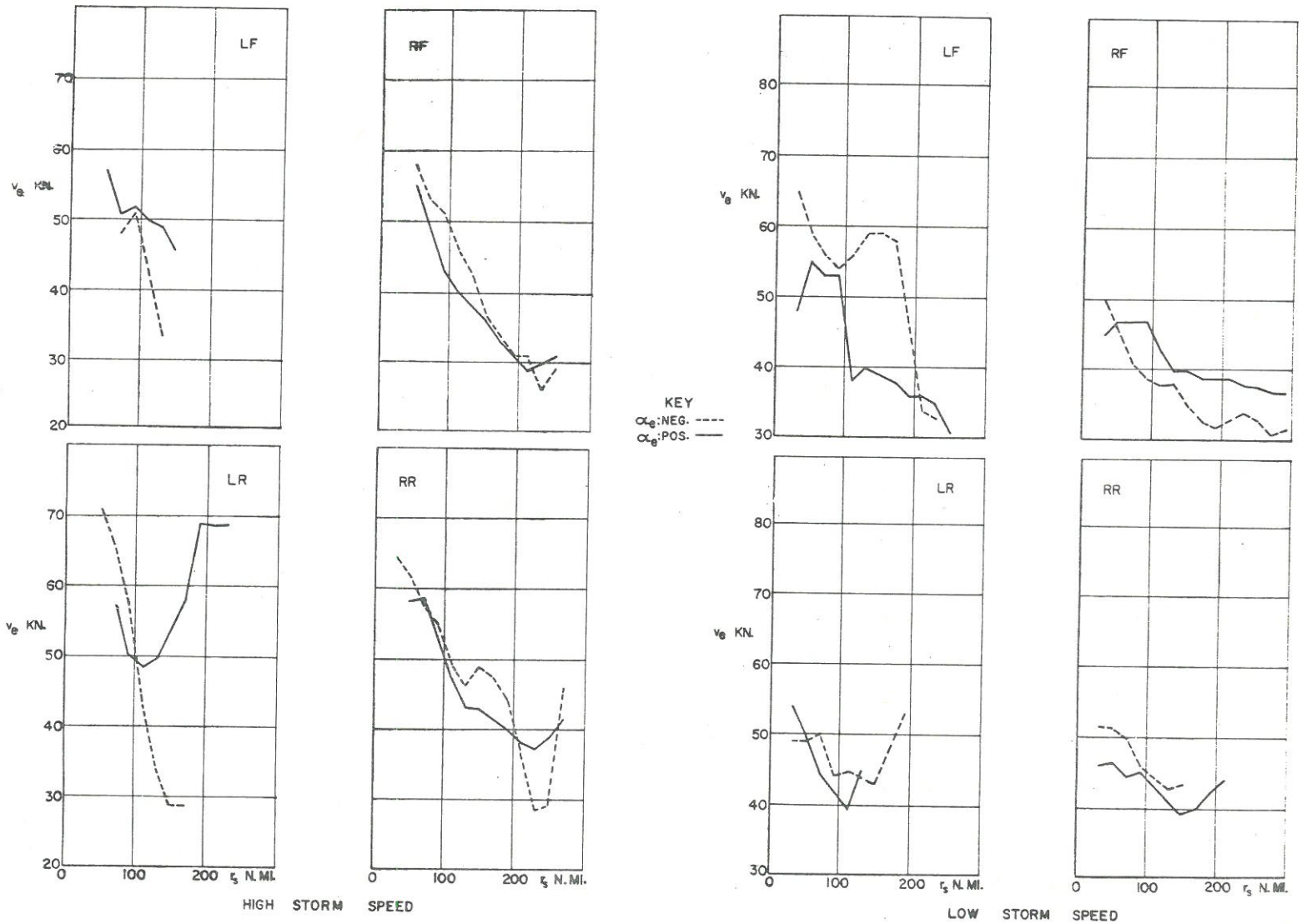

Figure 11. - Echo speed vs. range for signed crossing angles at high and low storm speeds in each quadrant.

It is interesting to note that in the left rear quadrant there are very few inward moving echoes at low storm speeds, and that at high storm speeds there are almost no outward moving echoes. If the procedure of subtracting the whole storm speed vector is correct[3], it would seem that for low storm speeds at all ranges greater than 150 n. mi. in this quadrant a condition of complete echo outflow exists. At high storm speeds the situation has reversed itself, and conditions of complete echo inflow prevail in the left rear quadrant.

Figure 12 shows the crossing angle of the Donna echoes plotted against range for high and low storm speeds in each quadrant. In all quadrants except the left rear, at all ranges and for all storm speeds, inward moving echoes have larger crossing angles than outward moving echoes. In the left rear quadrant at low storm speeds, outward moving echoes have much larger crossing angles than inward moving echoes. Outward moving echoes seem to have slightly larger crossing angles at most ranges in the left quadrants when the storm speed is low. Inward moving echoes at most ranges in the front quadrants have similar crossing angles at both high and low storm speeds. Inward moving echoes in the rear quadrants have their largest crossing angle values for low storm speeds.

Figure 13, a plot of radial echo speed vs. range for high and low storm speeds in each quadrant, is naturally dependent on the values of crossing angles. Thus the same conclusions apply as for figure 10.

Azimuthal Dependence of Parameters

Figure 14 is a graph of echo speed vs. azimuth for echoes with signed crossing angles at high and low storm speeds for three range intervals: "near" (40-60 n. mi. from the storm center), "mid" (80-100 n. mi.), and "far" (120-140 n. mi.). In all quadrants except one in these range intervals the echo speed is highest for high storm speed; (in the left front quadrant at the far range interval, inward moving echoes at high storm speeds have the lowest speeds). At high storm speeds it is concluded that: (a) in the near range interval inward moving echoes have higher speeds than outward moving echoes; (b) for the mid-range interval inward and outward moving echoes have nearly the same speeds; and (c) for the far range interval outward moving echoes have generally higher speeds than inward moving echoes.

At low storm speeds in the three range intervals, outward moving echoes generally move faster than inward moving echoes. It is apparent that: (a) for the nearest interval the arrangement of the four curves remains the same at all azimuths of the storm; (b) for the mid-range interval this is generally true, except in the left front quadrant at low storm speeds; and (c) in the farthest range increment no clear cut conclusions are apparent.

---

[3] Myers and Malkin [5] present a case for subtracting only part of the storm center motion in obtaining wind distributions about hurricanes.

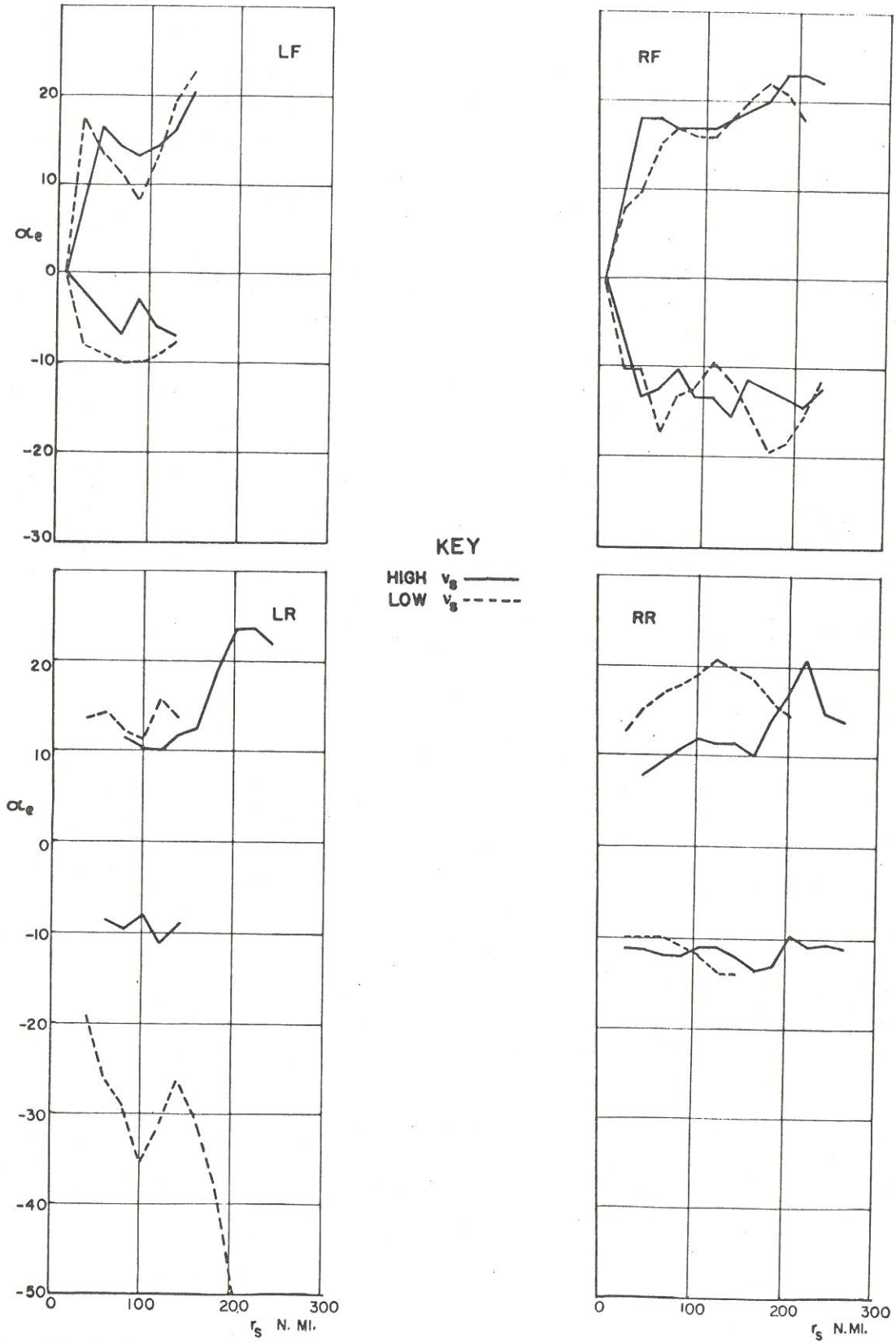

Figure 12. - Echo crossing angle vs. range for high and low storm speeds in each quadrant.

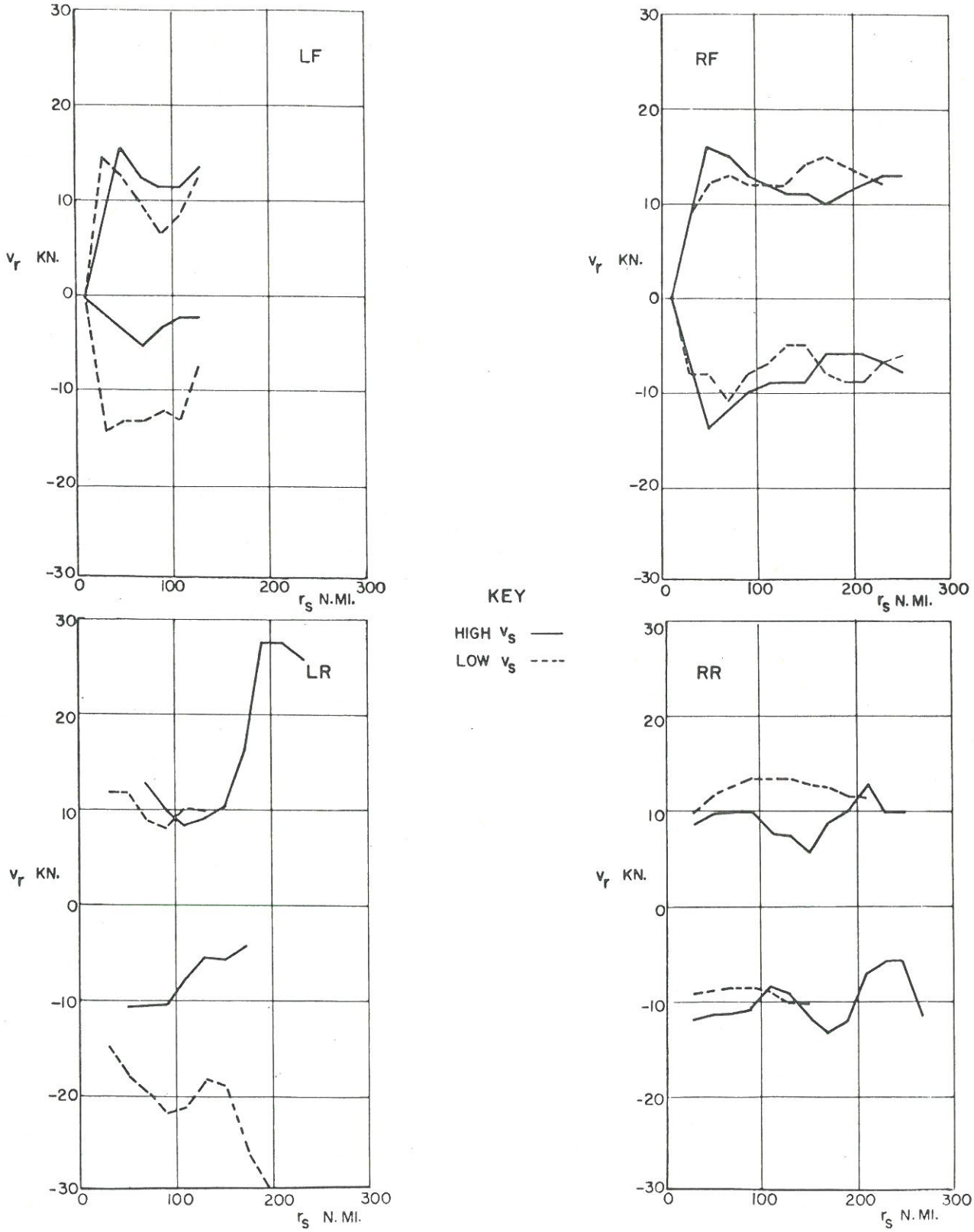

Figure 13. - Radial echo speed vs. range for high and low storm speeds in each quadrant.

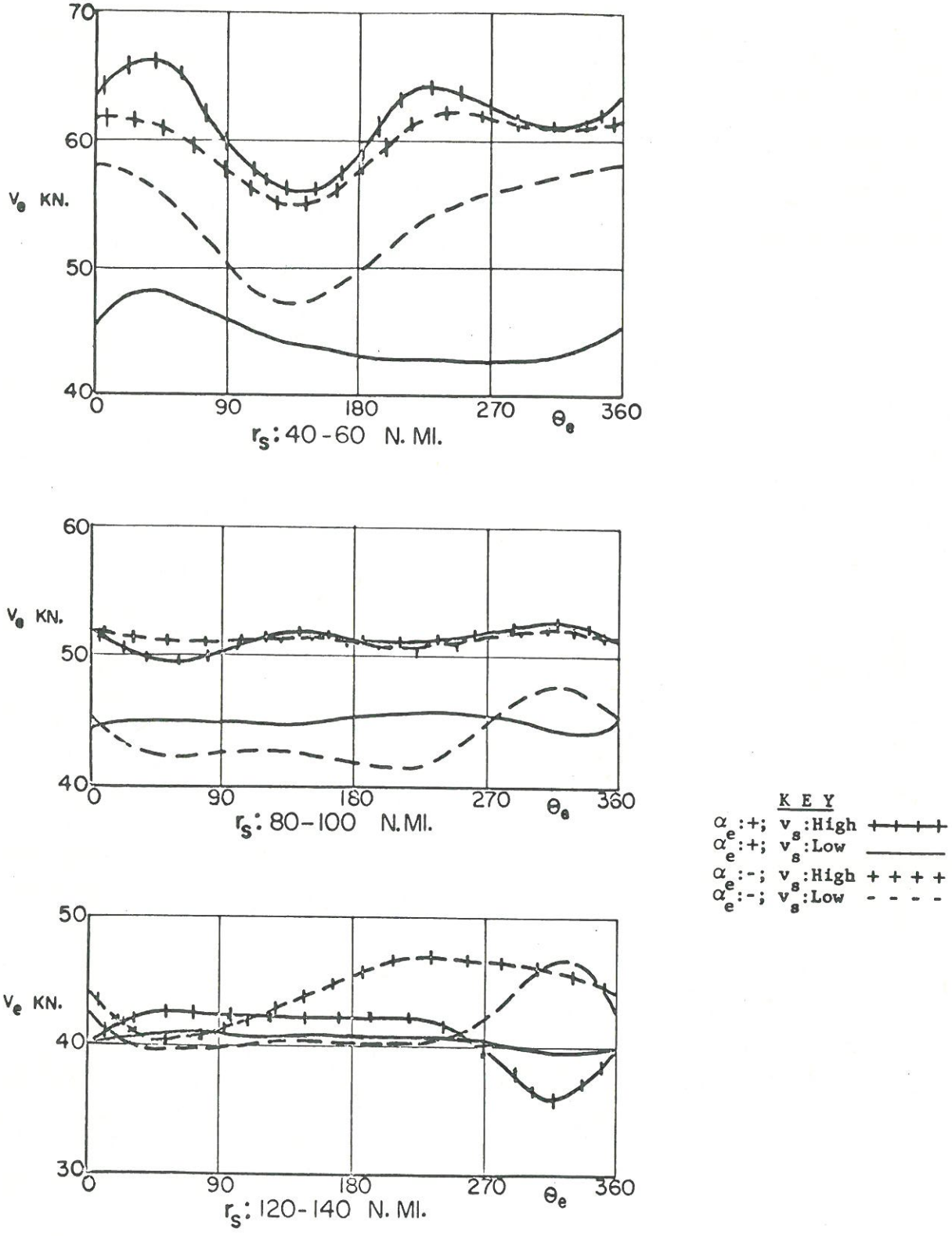

Figure 14. - Echo speed vs. azimuth for signed crossing angles in selected range intervals at high and low storm speeds, hurricane Donna.

Figure 15 shows echo crossing angle plotted against azimuth for three range intervals at high and low storm speeds. The following observations are pertinent: (a) the absolute crossing angles corresponding to low storm speed are generally greater than those corresponding to high storm speed (except for outward moving echoes in the right front, right rear, and left rear quadrants in the far range increment and outward moving echoes in the middle increment); and (b) inward crossing angles are slightly larger in value than outward crossing angles (except at low storm speeds at mid-ranges and the rear quadrants at high storm speeds in the nearest range increment, where the reverse is true).

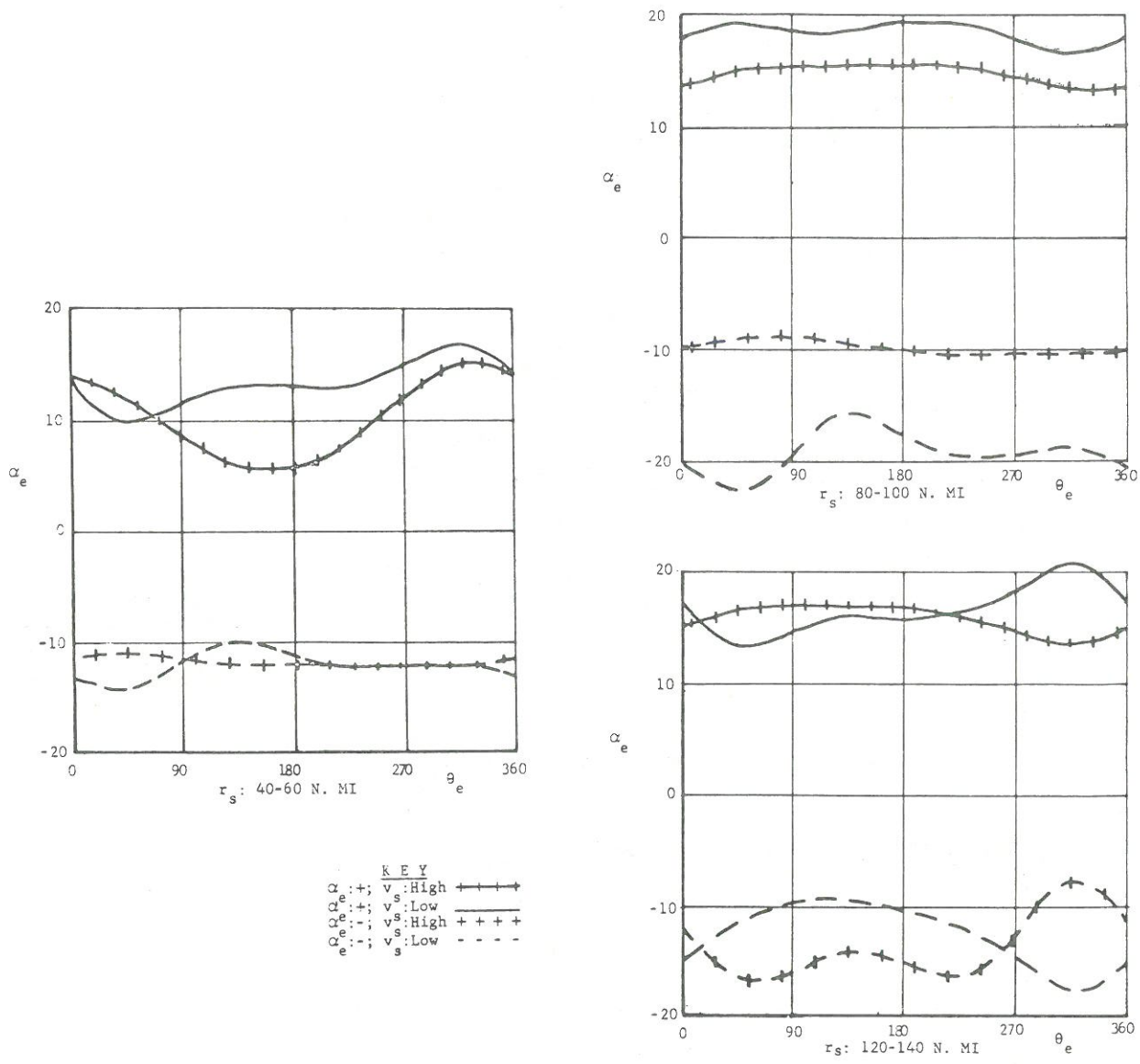

Figure 15. - Echo crossing angle vs. azimuth in selected range intervals at high and low storm speeds in hurricane Donna.

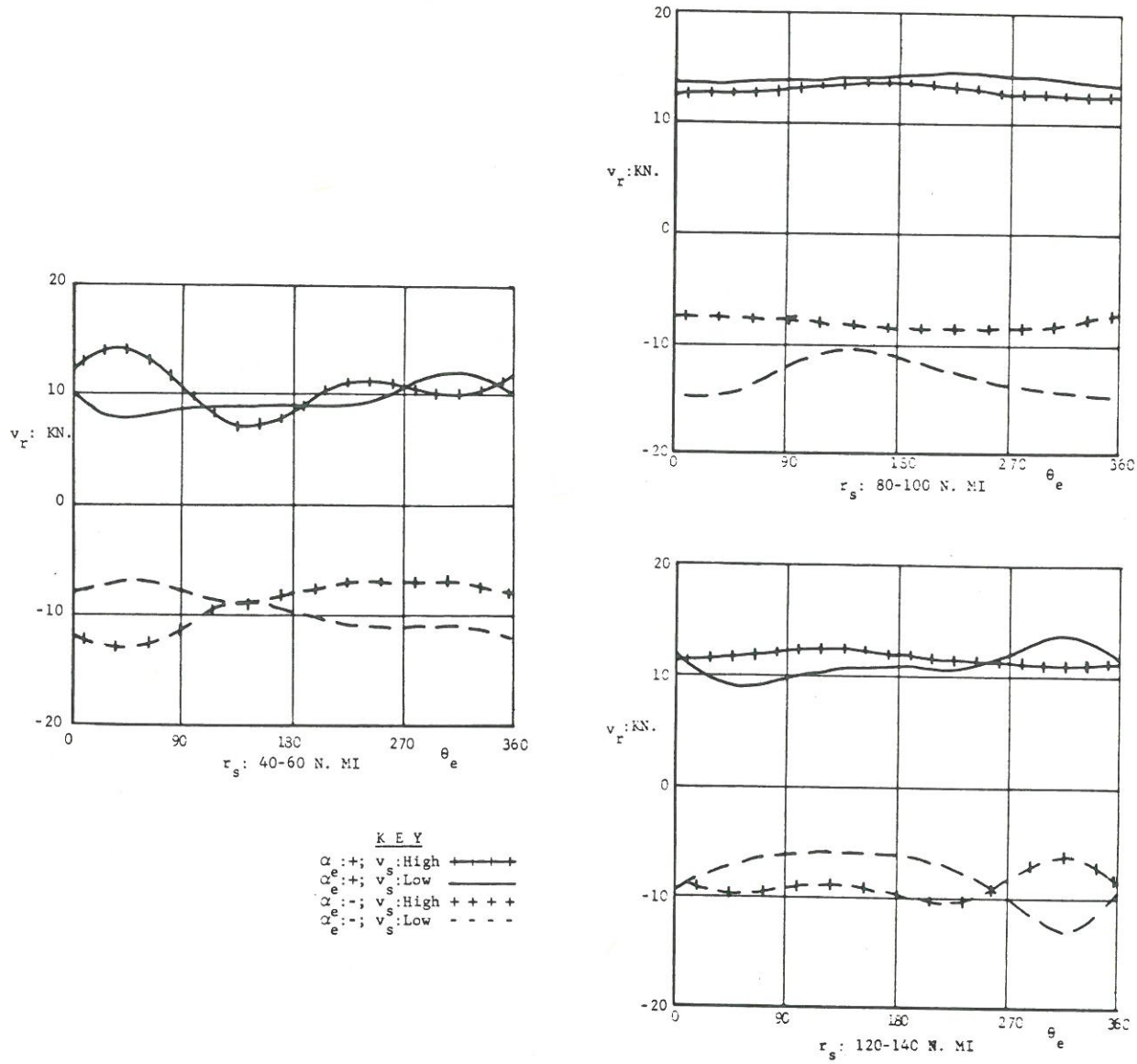

Figure 16. - Radial echo speed vs. azimuth in selected range intervals at high and low storm speeds in hurricane Donna.

Figure 16 shows radial echo speed vs. azimuth for three range increments at high and low storm speed. It differs from figure 15 in that v_e enters into its computation. The conclusions are, however, very similar to those for figure 15.

Environmental Dependence of Parameters

Echo Motion Over Land and Over Water - The differences in the effect of the land and water environments on the echo motion were studied by dividing the Donna echo data into four categories by the following scheme:

I. Over-water; before 0000 EST, September 10;
II. Transition I; from 0000-0800 EST, September 10;
III. Transition II; from 0800-1600 EST, September 10;
IV. Over-land; after 1600 EST, September 10.

Approximately one-third of the echoes in Donna appeared over water, one-third over land, and one-sixth in each transition period. The location of the storm during each of these periods is shown in figure 1, a plot of the hurricane track on September 9-10, 1960.

Figure 3 indicates that Donna was moving slowly over water and increased in speed over land. Consequently, both the over-land low storm speed and the over-water high storm speed categories have very few echoes. In order to facilitate land-water comparison, the medium storm speed case is presented in figure 22 and 24 for echoes with positive and negative crossing angles. The summarized land-water comparisons are also presented for all α_e and v_s in figure 23 and 25.

An attempt was made to plot the distribution of echoes in the various categories. Considerable bias was present in the location of the radars with respect to the storm center at the time the echoes were traced. Consequently, only these very tentative conclusions could be drawn: (a) most echoes are found nearer the storm center when the storm was over land, but there is a more even distribution of echoes to greater ranges when it was over water; and (b) when Donna neared land, it quickly assumed the echo characteristics of the over-land type with very little "transition".

Figure 17 shows v_e vs. r_s for v_s medium and $\pm$ α_e, and figure 18 shows v_e vs r_s for all v_s and α_e. Since Donna's speed was generally low over water and high over land, figure 18 is biased so that v_e over land is greater than it is over water. However, figure 17 is considerably less complicated since the storm speed and crossing angle bias have been eliminated by plotting all sections of the figure using only one value for each of the variables v_s and α_e. Figure 17 shows that inward moving echoes move faster over land than over water, within about 100 n. mi. from the storm center in the right quadrants. This conclusion is verified by figure 18 despite storm speed bias.

The situation in the left quadrants of figure 17 is considerably more complicated. The echo speeds in transition I are also lower than those in transition II, although the transition II echo speed exceeds the over-land echo speed in the rear quadrants.

Figure 19 shows the change in crossing angle with range from the storm center for v_s medium (positive and negative crossing angles only). There appears to be a slight increase in α_e with range from storm center, as we would have expected from previous data. However, echoes in the front quadrants over land seem to have few significant differences in crossing angles

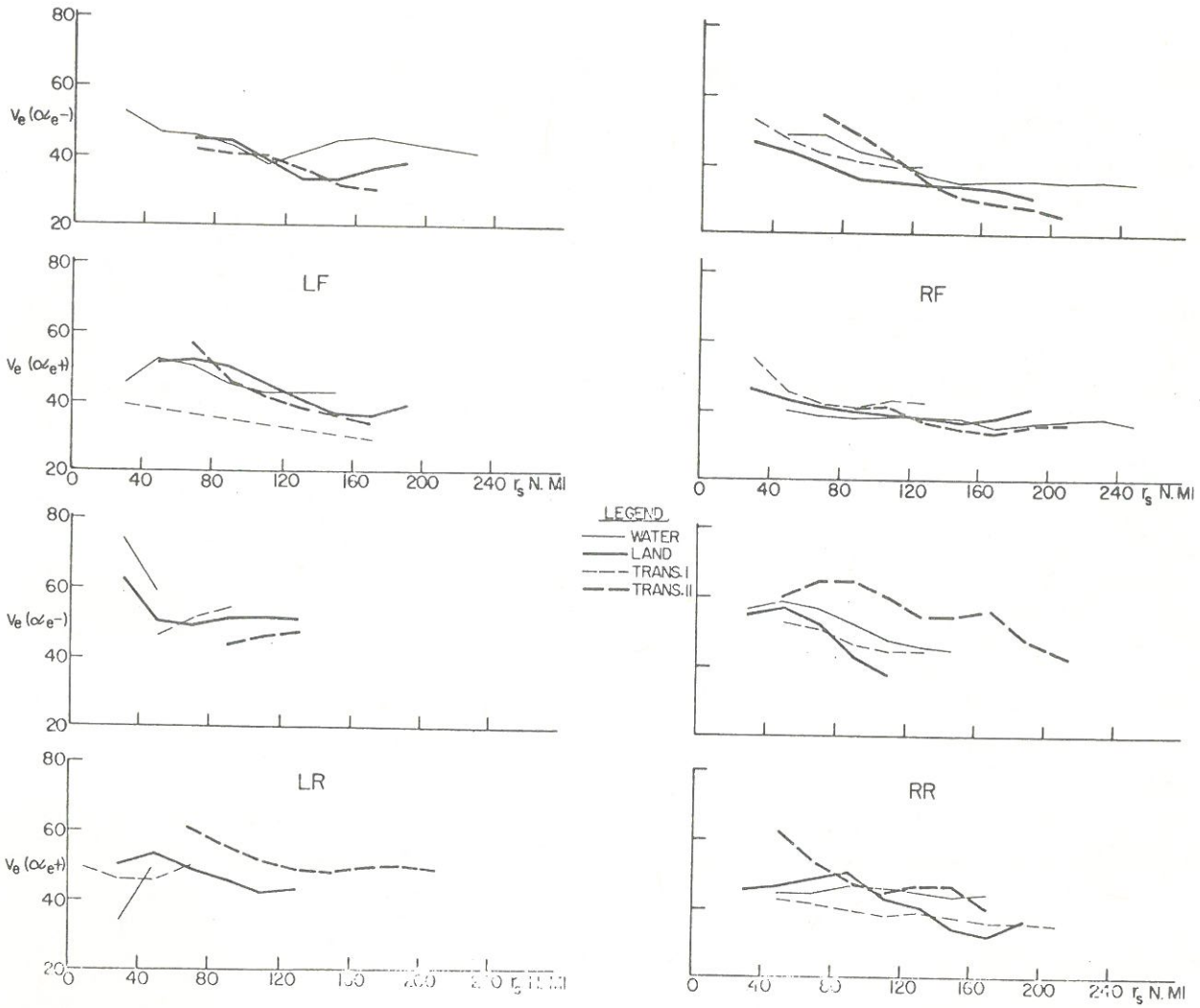

Figure 17. - v_e vs. r_s over land and water for medium v_s and $+\alpha_e$ (3 point running mean)

compared to those over water. The over-water echoes have larger crossing angles in the right rear quadrant.

Figure 20 shows absolute α_e for all α_e and v_s. The curves are remarkably similar for the front quadrants. The right rear quadrant shows a definite tendency for over-water echoes to have larger crossing angles than those over land, beyond 100 n. mi. from the storm center. In the left rear quadrant the average absolute crossing angle for over-water echoes is almost twice that for over-land echoes. These conclusions must be viewed in the light of the data sample characteristics where it can be shown that the over-water crossing angles in the left rear quadrant are very few in number, possibly reducing confidence in them.

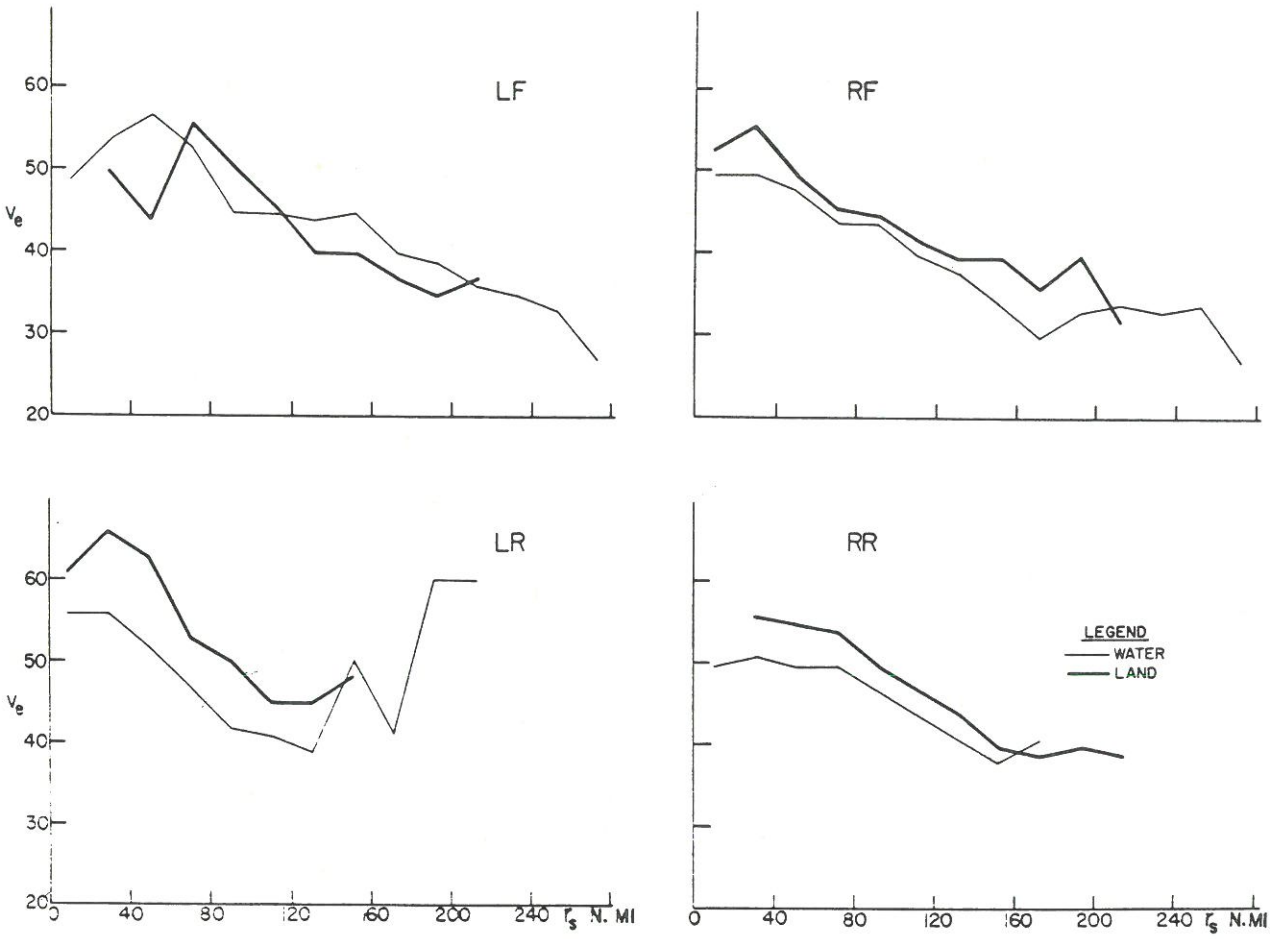

Figure 18. - v_e vs. r_s over land and water for all v_s and α_e.

Despite the fact that considerable bias is inherent in the data, the above study has led to the following tentative conclusions: that the maximum concentration of echoes is generally found closer to the storm center when the storm is over land than when it is over water; and that, at least in the rear quadrants, the echoes are moving faster and with slightly smaller crossing angles while the storm is over land.

Echo Motion - Day and Night - For this study the Donna echo-card data were divided into three groups:

I.	Day;	0900-1700 EST
II.	Night;	2100-0500 EST
III.	Transition;	0500-0900 and 1700-2100 EST .

Approximately one-half of the echoes appeared in the transition category and one-fourth in each of the others.

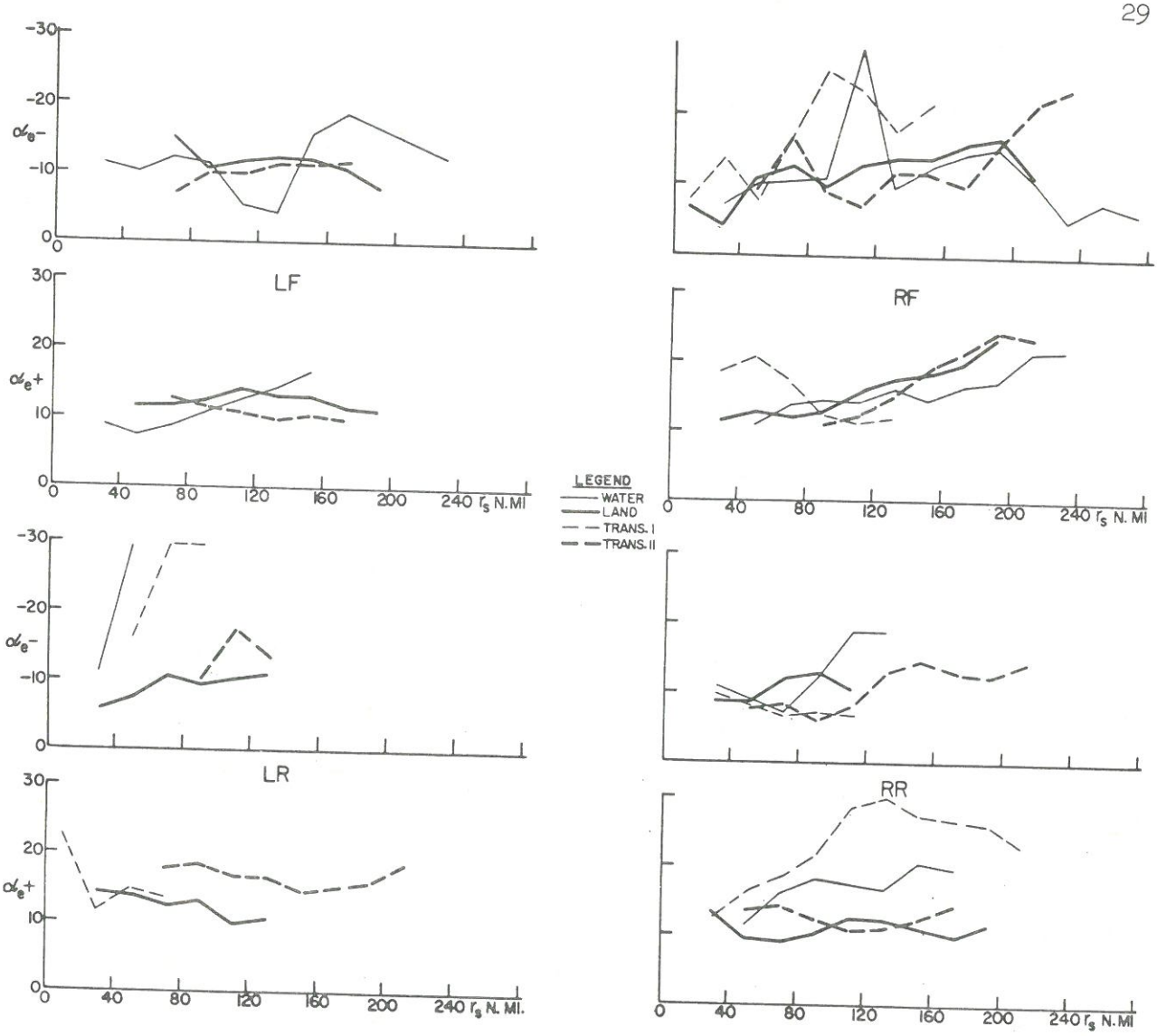

Figure 19. - α_e vs. r_s over land and water for medium v_s and $\pm$ α_e (3 Point running mean)

Radar bias is minimized in this study since both Miami and MacDill radars see echoes during both day and night periods. The day echoes on September 9 are subject to the same conditions. On September 10 the day echoes were seen by both University of Miami and MacDill radars and appear mostly in the right and front quadrants; night echoes on September 10 are from the MacDill radar. It is clear that each radar viewed the storm through one day-night cycle without any very great change in the orientation of the storm with respect to the radar. Thus we can discuss the results without reference to radar location.

In the discussion of the land-water study, the medium storm speed, positive crossing angle case was presented for specific reasons. In this section the presentation is again confined to one or two specific cases

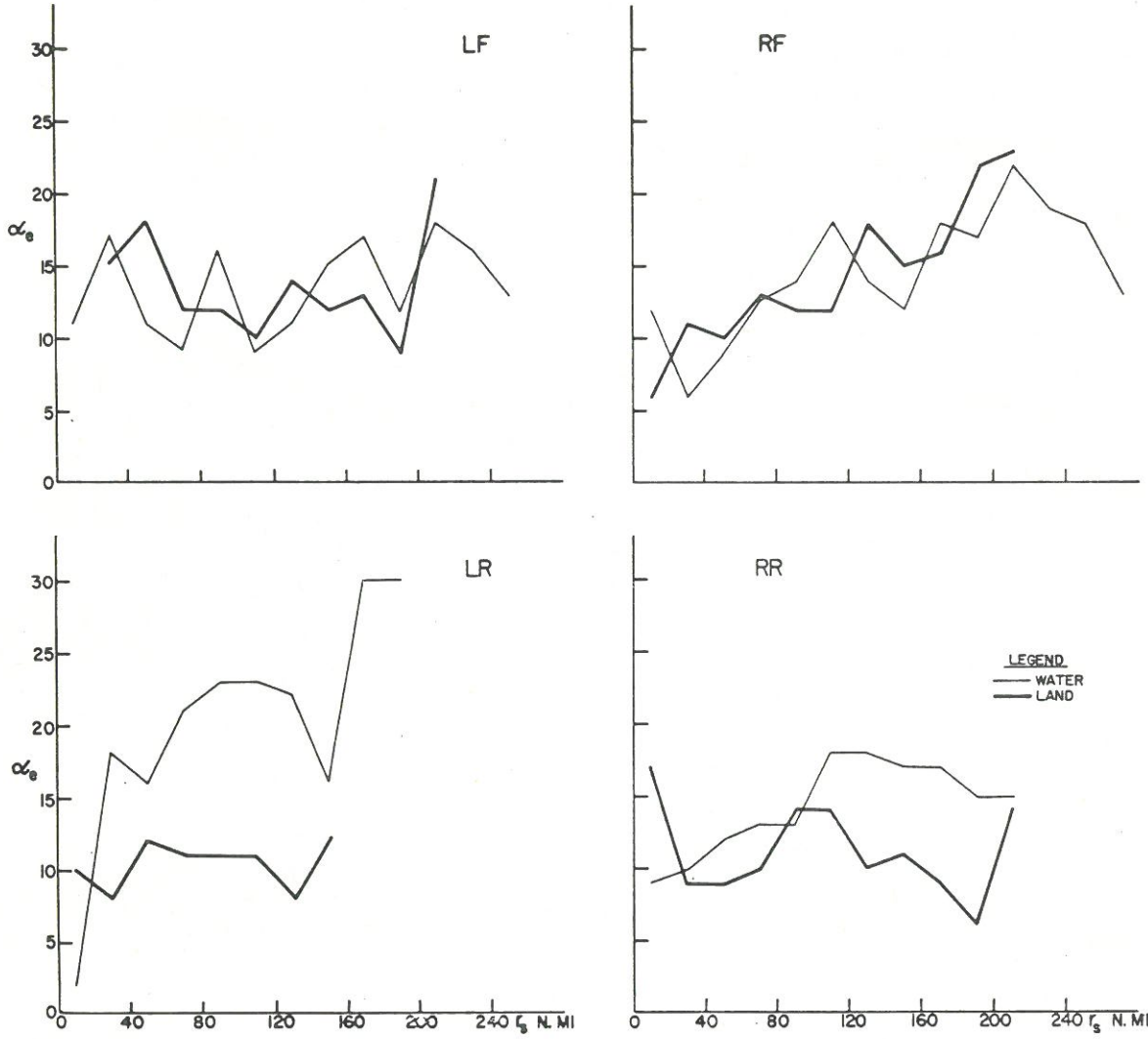

Figure 20. - α_e vs. r_s over land and water for all v_s and α_e.

rather than all cases, since the data are rather voluminous and the reader would probably be confused rather than enlightened by a complete presentation. The low storm speed, positive crossing angle case was selected because it seemed representative of the variety which appeared in the specific cases.

Plots were made of the fraction of echoes in each 20-n. mi. r_s increment as well as α_e. It was apparent that most of the night echoes are found at shorter r_s than the majority of the daytime echoes. From the echo distributions the storm thus appears smaller at night than during the day; but the normal daytime eccentricities in echo distribution about the storm center are found at night as well as in the daytime. It should be pointed out that a change in the <u>type</u> of predominant echo from day to nighttime, rather than the <u>distribution</u> of the field of echoes, could also produce the above results. Although the statistical results would be the same, the meteorological mechanisms responsible for each could be very different.

Figures 21 and 22, echo speed vs. range for v_s and α_e and for all v_s and α_e respectively, show that the echo speeds at night are slightly lower than during the day.

Figures 23 and 24, positive crossing angle vs. r_s for v_s low, and absolute crossing angle vs. r_s for all v_s and α_e respectively, show that the crossing angles at night are equal to or smaller than those during the day. This is an expected consequence of the apparent decrease in storm size and shows that the storm is more symmetrical at night.

The question of radar bias entering into this study has already been discounted. However, possible bias arising from storm location with respect to land-water must be accounted for in any discussion of land-water and night-day results. During the day and night of September 9 the storm was over water; during the day on September 10 the storm was either over land or in the transition II category; at night on September 10 the storm was partly over water and partly over land. Therefore the day category is divided between over-land and over-water echoes, while the night category consists of a majority of over-water data. It appears that the day and night categories are divided between land and water echoes so that bias from one or the other should largely cancel out.

Looking at the land-water study from the point of view of day-night bias, it can be seen that the over-water categories are evenly divided between day and night, canceling out bias in this category. The over-land categories consist primarily of night and transition echoes. Some of the transition echoes would serve to counteract to some extent the effect of the night echoes, but there does exist a clear bias in this case. The conclusions of the land-water study, already questionable because of radar bias, are now made even more amorphous as a result of a night bias in the over-land category. The day-night study, however, is found to be almost completely without bias.

The Dependence of Echo Motion on Height

Although no good time-lapse CAPPI (Constant Altitude PPI) radar data are available for hurricanes, it has been one of the aims of this project to determine the variations which might exist in echo motion with height. This, with simultaneous wind data from NHRP flights, could lead to a separation of advective and propagative echo motion components, and also provide further insight into the energy processes involved in echo growth and decay. Since such data are non-existent (even the usual vertical cross sectional RHI photographs are rare for hurricanes on a time lapse basis), we attempted to use the voluminous Donna data to study variations in echo motion with height.

In the present studies the height of the volume in space that is being sampled by the radar pulses is a known function of range (assuming normal propagation and constant 0° antenna elevation angle). The radar beam automatically integrates a rather large interval of height, and the radar-scope shows the maximum (detectable) reflectivity cross section of any integrated echo. Actually, the echo itself may extend above and/or below the beam limits (defined at the half power points) or may be entirely

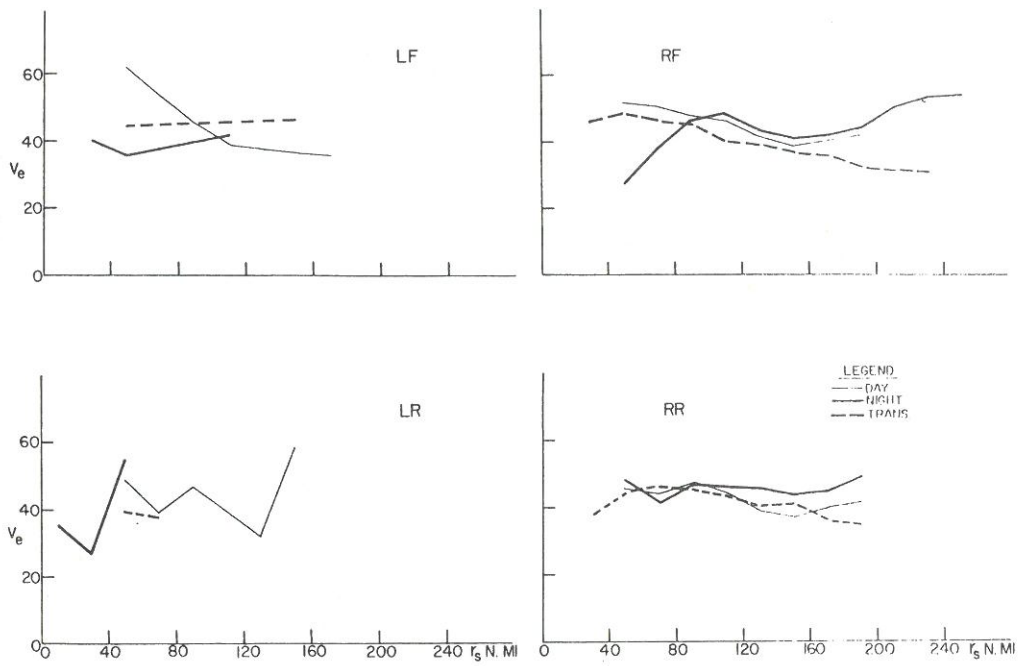

Figure 21. - v_e vs. r_s day and night for low v_s and $+\alpha_e$ (3 point running mean).

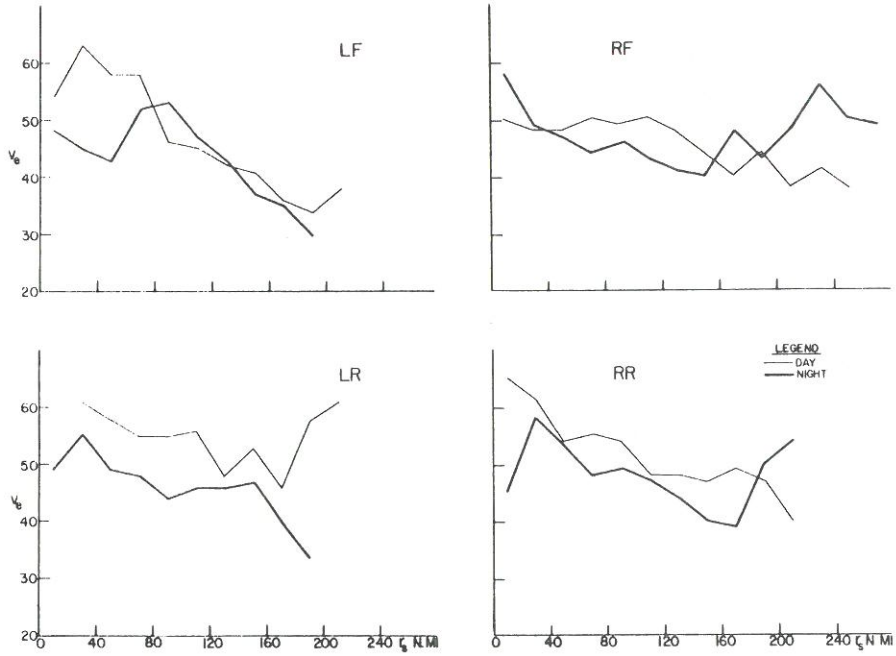

Figure 22. - v_e vs. r_s day and night for all v_s and α_e.

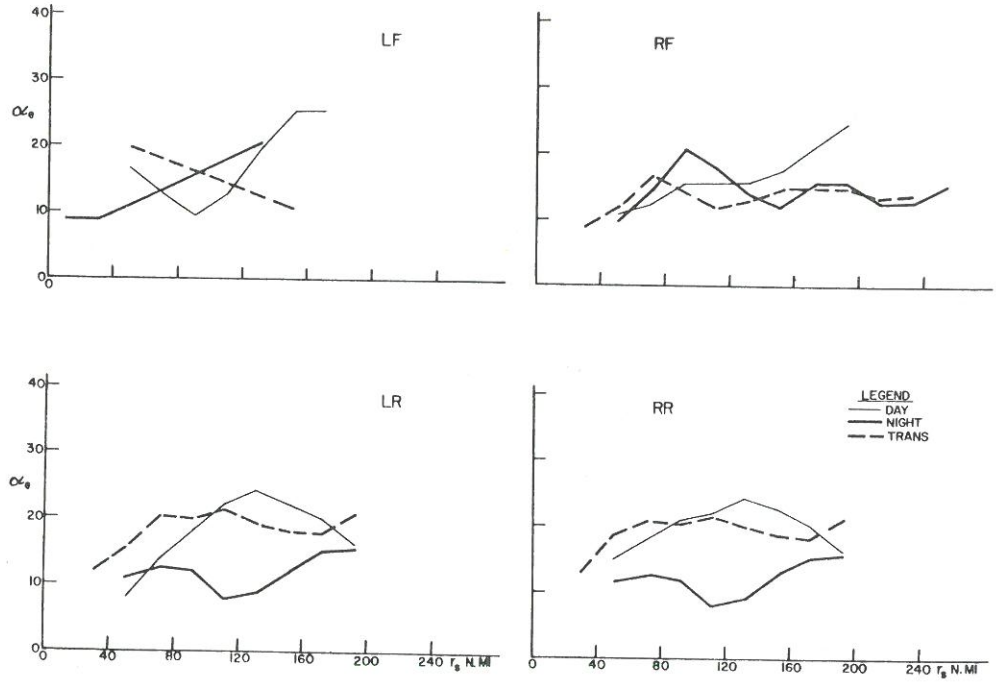

Figure 23. - $\alpha_{e_{mean}}$ vs. r_s day and night for low v_s and $+\alpha_e$ (3 point running

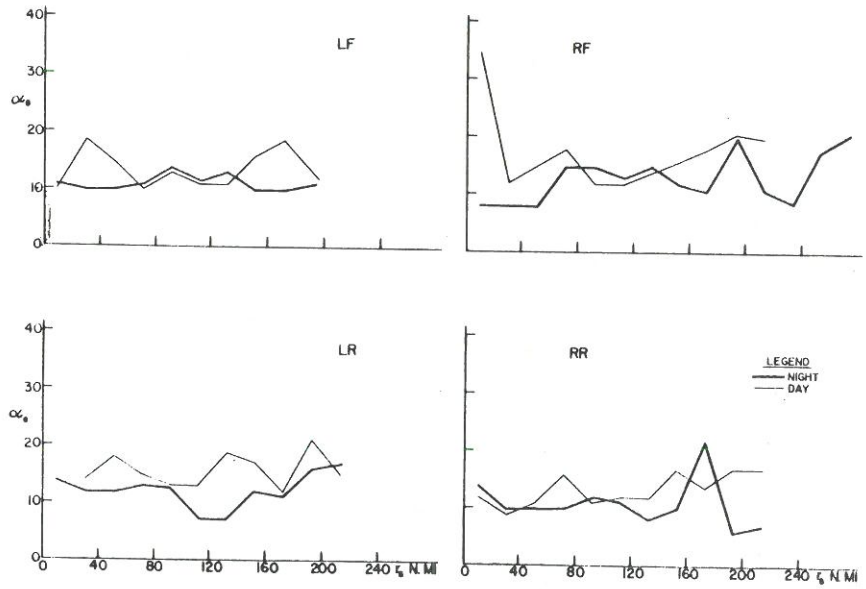

Figure 24. - α_e vs. r_s day and night for all v_s and α_e.

enclosed within these limits. This makes it very difficult to assign an "average height" to the echoes. Furthermore, the motion of the echo is the resultant of vector winds over its entire height, considered together with growth factors, and thus may be primarily the result of conditions occurring outside the limits of the radar beam. Clearly, the results of such a study could be expected to be amorphous at best.

Indeed, the over all results are completely inconclusive, although there appears to be a tendency for echo speed and crossing angle to decrease with increasing r_r regardless of r_s. Such results correlate somewhat with NHRP wind print-outs which show, at least for the inner hurricane regions, a general decrease of wind speeds with height and a more circular wind pattern with less inflow in the middle levels as compared to lower levels.

The Dependence of Echo Speed on Crossing Angle

Some sort of dependence of echo speed on crossing angle was indicated in the initial study of Donna data [13]. Accordingly, the data were sorted and listed and the average echo speed obtained for 10° intervals of crossing angle. The v_e vs. α_e was plotted in figure 25 for three separate range increments. A plot of n vs. α_e is also shown so that confidence levels may be established for the data.

Figure 25 shows a definite linear relationship between echo speed and crossing angle. In general the line has a positive slope in the front quadrants (i.e., inward moving echoes move faster than outward moving echoes), and a negative slope in the rear quadrants (the opposite case) for all storm speeds. This is a more conclusive result than that described in Radial Dependence of Parameters, where the data were somewhat confused on this point.

The variation of echo speed with crossing angle can thus be represented to within $\pm$ 15 kt. accuracy by the equation

$$v_e = \pm \frac{1}{6} \alpha_e + 44$$

where the plus sign of the slope is associated with the front quadrants and the minus sign with the rear quadrants.

Echo-Wind Kinematics

Figure 26 shows the 1800 GMT surface winds in the region of Donna, along with some of the 1,600-, 13,000- and 14,200-ft. winds from NHRP flights between about 1400 and 2000 GMT on September 9, 1960. Radar echo data for 1700-1900 GMT are superimposed on the wind data for comparison. Although some of the differences in time for the various data are obvious, certain general inferences can be made. The surface winds, as one might expect, have greater inward crossing angles than other winds or echoes in the same vicinity. The magnitude of the crossing angles is suprisingly great even for surface winds, 75° for one and 60° for the other observation within 75 n. mi. of the storm center. The 1,600-ft. winds are essentially tangential in the left front and right rear quadrants, outward in the left rear quadrant, and appreciably inward in the right front. The 13,000- and

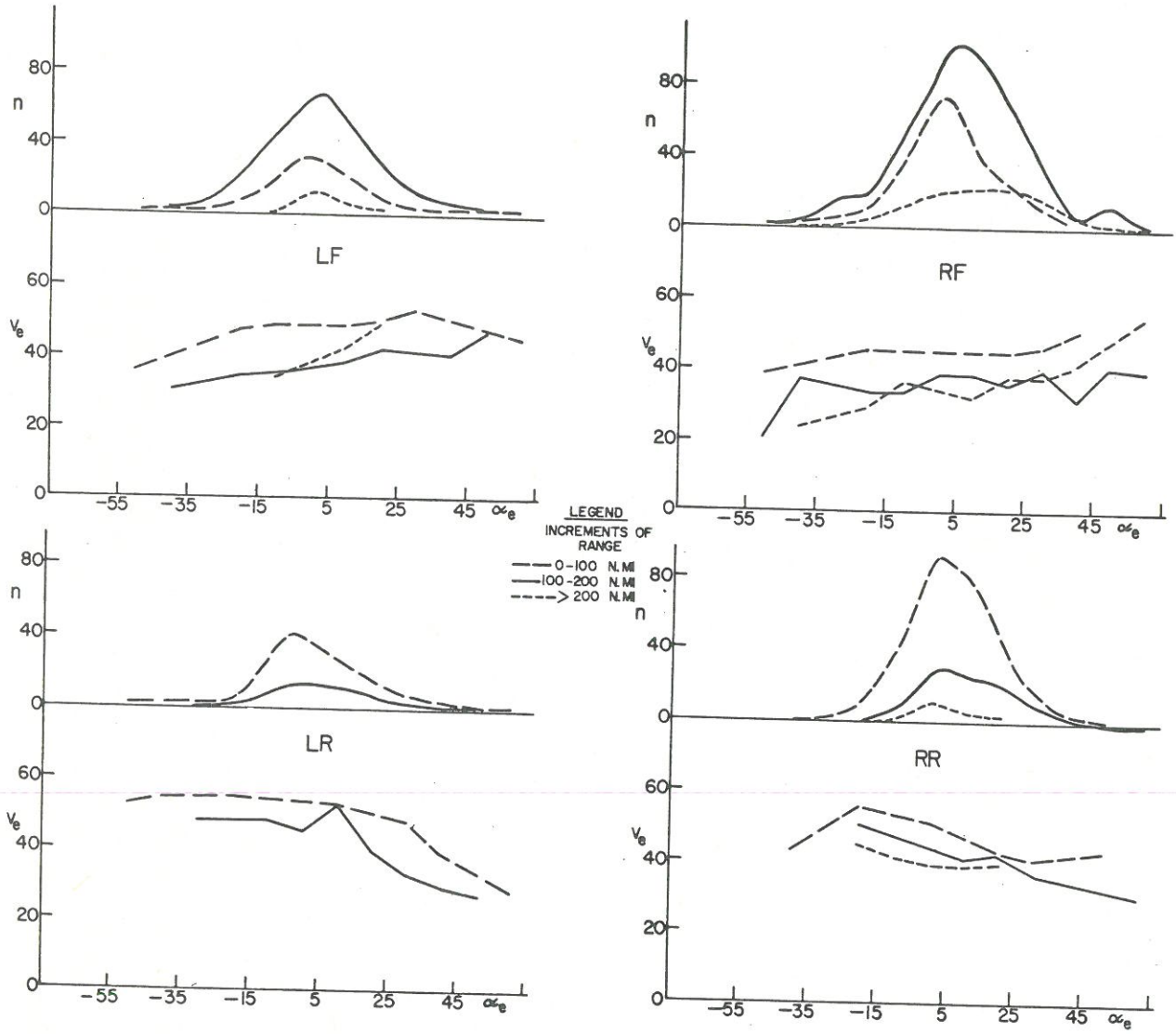

Figure 25. - v_e and n vs. α_e for medium v_s at r_s = (0-100), 100-200), (> 200) n. mi. (3 point running mean)

14,200-ft. winds are essentially tangential with very small outward radial components in most quadrants. Unfortunately, the storm center was so far from land that echoes are representative of only the right quadrants and the left front quadrant.

Echoes in the right front quadrant have inward crossing angles of smaller magnitude than those of the 1,600-ft. winds, and about the same crossing angles as the 14,200-ft. winds; but their speeds are generally lower than the winds at all levels plotted in figure 26 near the storm center. However, in the right front quadrant echoes at greater ranges generally exceed the wind speeds.

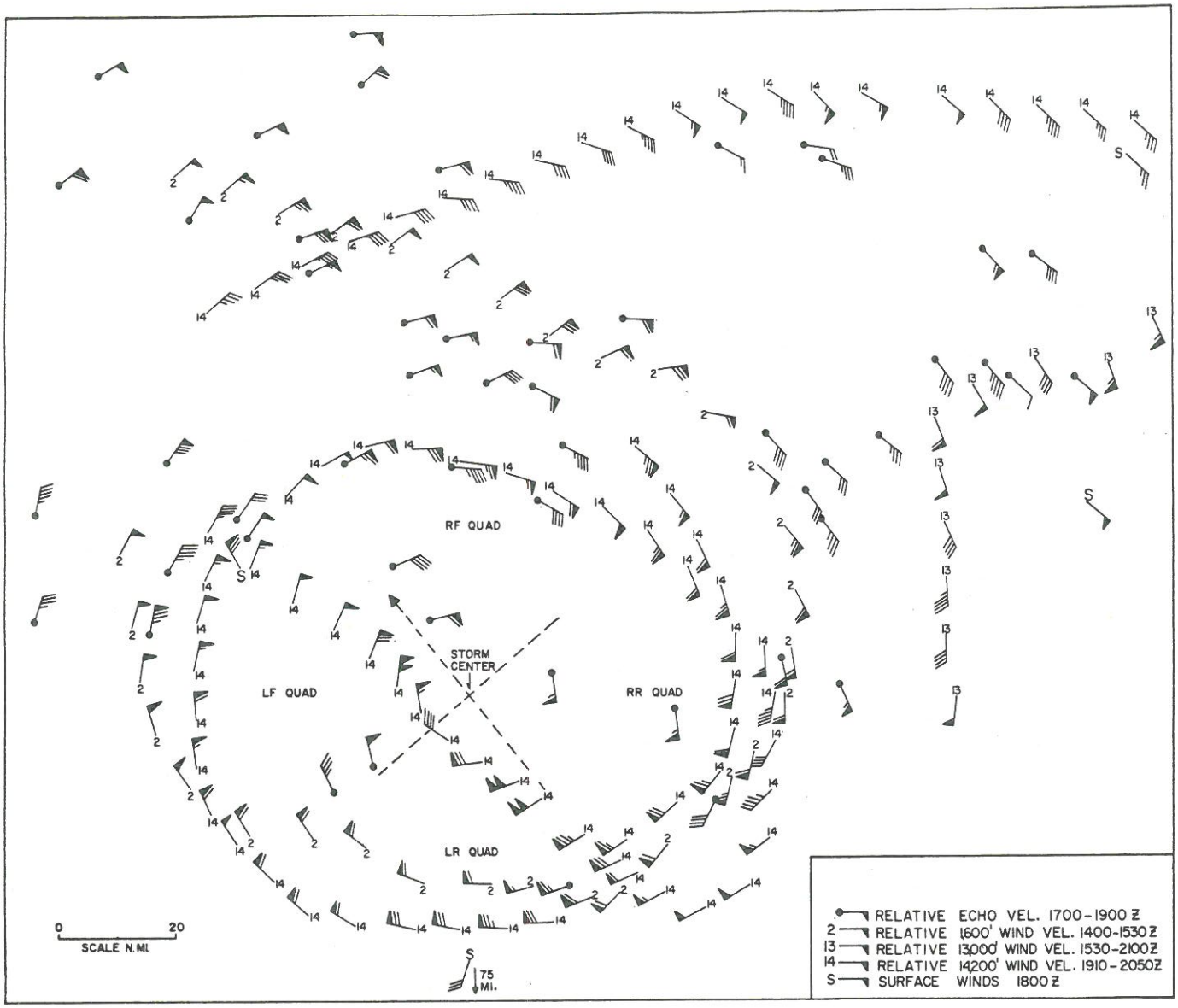

Figure 26. - Echo and wind velocities hurricane Donna, September 9-10, 1960.

Echoes in the right rear quadrant have greater inward crossing angles than all the winds plotted but their speeds are near the wind speeds.

Echoes in the left quadrants more nearly approximate the wind speeds and directions at both the 1,600- and 14,200-ft. levels. (There appear to be few differences between the winds at these two levels in this region.) Almost all echoes and winds plotted are nearly tangential, i.e., they have small inward or outward crossing angles.

Although height data are not available for all the echoes shown in figure 26, RHI data for the region of the right quadrants taken a few hours later show a widespread "bright band" at 17,000-18,000 ft. as in figure 27. The bright band, an indicator of the melting level, was higher by 1000 to 1500 ft. when found in Donna than is usually the case in the Miami area. Its presence is widely thought to indicate mature or decaying convective systems and general stability. The average convective echo tops in the right front quadrant exceeded the 13,000-14,000-ft. wind levels by 6,000-10,000 ft. Echo bases were not available because of distance and earth curvature effects. The bright band was not present earlier on September 8 in the regions of pre-hurricane squall lines or outer convective activity; nor was it present later on September 10 in the region of spiral band tails in the far right rear quadrant. Thus, it appears that the rainshield and most inner regions of the hurricane Donna precipitation pattern (at least in the right quadrants) were relatively stable compared to the inner "core" and the "outer convective region." PPI observations have long led to the same conclusion where the rainshield was called the "graveyard of spiral bands" [8].

The data in figure 26 indicate slightly less wind shearing with height in the left quadrants than the right. Some RHI data are also available for further study of echo motion at various heights, and allied studies of the problem with the present IBM echo data are now in progress. There is a growing conviction that the hurricane echo-wind relationship is severely complicated by propagation components. Since evidence exists that small radar precipitation echo areas do not necessarily move exactly in accord with the wind at a particular level, or even with the integrated winds through the layer in which the echo is embedded, the term "spa-wind" [4] would be inappropriate and possibly misleading in such cases. The possibility of relating echo-motion to integrated environmental wind is not a bright one. The question of the effects of propagation on such a relationship is sufficiently indeterminant to void any clear cut conclusions at this time.

The present hurricane Donna echo distribution should be at least partially duplicated with data from other storms when better simultaneous radar and wind data become available. Even though such studies are time consuming, it is necessary that they be repeated in order to determine the true kinematic echo-wind relationships for both hurricane and other tropical weather situations.

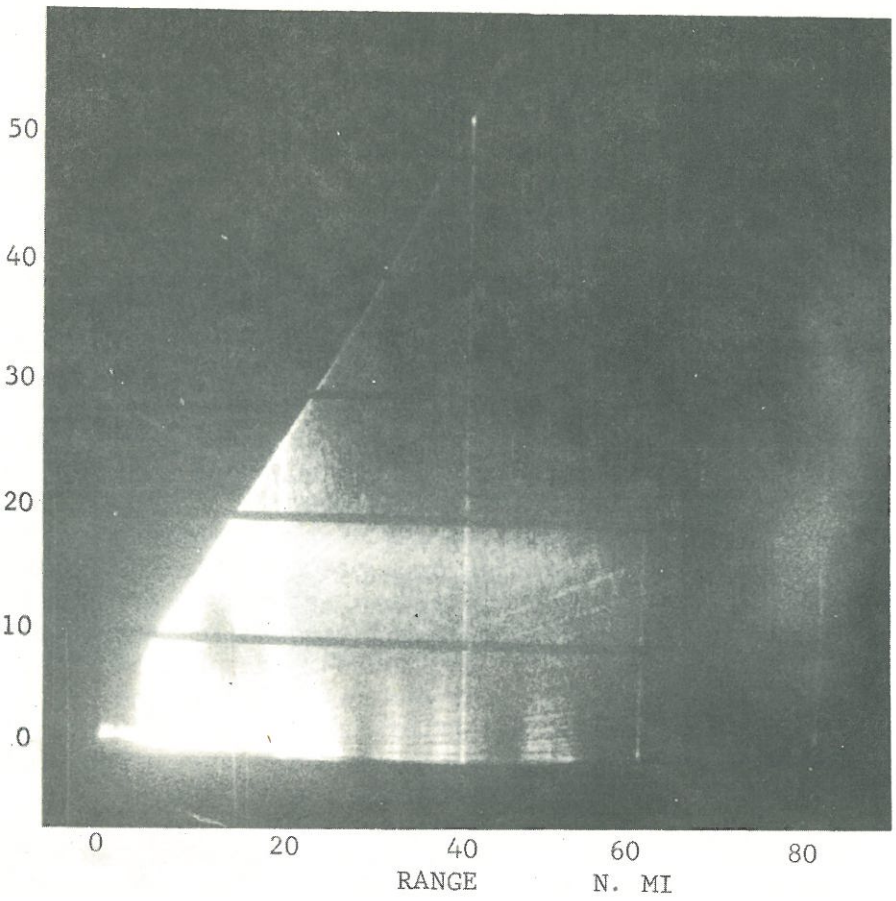

Figure 27. - "Bright band" in hurricane Donna, 1655 EST September 9, 1960. University of Miami MPS-4 RHI scope, 1.3 sec. pulse, 164° azimuth. Precipitation attenuation is evident.

Hurricane Echo Lifetime and Diameter

Echo Lifetime - Echo lifetime (L_t) was studied for several hundred echoes in 1958 [9], but was not plotted against range or azimuth from storm center at that time. An average L_t of about 35 min. was indicated in that study.

It was originally planned to include such a study as part of the Donna work; but the increase in time and effort required to provide this information in the initial tracing of the Donna echo motion data made it necessary to drop this objective. The average time for which the echoes were traced was about 17 min. and consisted of four or five 5-min. traced echo outlines. This L_t, which appears on the cards for each echo, was usually the same for all echoes (up to 57) on a given tracing and can not be used to infer the actual L_t of either the individual echo or the group.

In lieu of the above, a special case study of L_t and echo diameter (d_e) as functions of range from the storm center, quadrant, and storm speed was performed. The data consist of 125 distinct, relatively circular echoes independently derived from the MacDill film of Donna. Echoes which were distinct throughout their lifetime were selected and carefully traced through the entire duration of their existence in the horizontally directed (but vertically wide) radar beam. The parameters of the study were L_t and d_e at the midpoint of the echo track.

Figure 28 shows a plot of L_t vs. r_s and quadrant. In all quadrants L_t decreases with increasing range from the storm center. For instance, echoes in the right front quadrant have lifetimes of 40-45 min. at a range of 80-90 n. mi. from the storm center and lifetimes of 20-25 min. at ranges greater than 160 n. mi. Data for the other quadrants were not so complete but the curves are consistent except for the left rear quadrant, which levels off to a lifetime of 35-40 min. at ranges past 120 n. mi. Echoes in the left quadrants have generally longer lifetimes than those in the right quadrants, with those in the left front quadrant existing longest of all. The echoes have greater lifetimes at high storm speeds than at low or medium storm speeds up to ranges of 160 n. mi. past which there is no clear storm speed dependence.

The mean L_t of about 35 min. of this study appears to support previous results, but the decrease in L_t with range from the storm center was not anticipated. The increasing height of the radar beam with range from land-based radars and the decreasing detection capabilities with increased range could combine to produce the general rapid decrease in L_t with range shown in figure 28 if the radar were located near the storm center. Although the radar was relatively close to the storm center, it was located far enough away so that the results cannot be accepted at full face value.

Echo Diameter - There does not appear to be any clearly defined dependence of echo diameter on range and quadrant, other than an unpredictable oscillatory one. Echo diameter seems to decrease with increasing range from the storm center at high storm speeds, from maxima of 6-6.5 n. mi. at 90 n. mi. range to minima of 4.25-4.5 n. mi. at 180 n. mi. range. But for low and medium storm speeds, the echo diameter appears to increase with range up to about 200 n. mi., and to decrease outside this range. The average diameter is about 5 n. mi., except in the right front where it is about 6 n. mi.

Donna Echo Data Compared with Data From Other Storms

The other studies of hurricane radar echo parameters that may be compared with this work are those performed by the authors in 1960 and 1961 [7], [13]. The data used in one of the studies were a group of about 600 echoes from hurricane Debra 1959. Hurricane Debra was much smaller than Donna and all the Debra data were within a range of 70 n. mi. of the storm center. Furthermore, the Debra data were not separated with regard to sign of crossing angle or storm speed, thus various kinds of statistical inconsistencies were introduced into the computations. It is therefore difficult to tell whether some of the minor differences are significant.

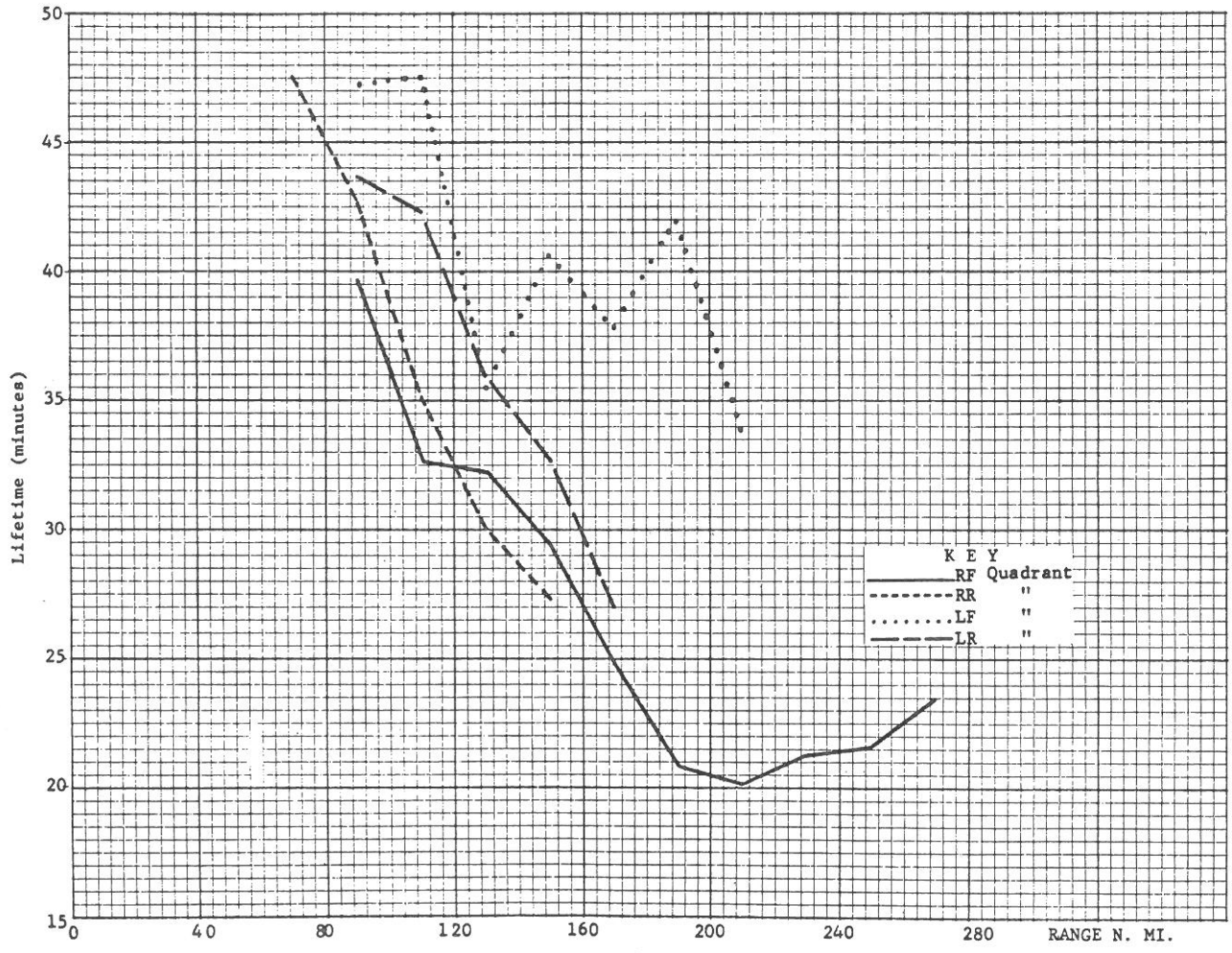

Figure 28. - Echo lifetime vs. range in each quadrant.

This study showed a hump in echo speed at a range of 35 n. mi. in the left front quadrant, a feature also apparent in the Donna data. The Debra 1959 data also supported the general conclusion that the fastest echoes are found to the left of the storm center. In fact, the general conclusions from the 1961 study regarding number of echoes to be found in various parts of the hurricane are also true for the Donna echo motion data. These and previous results have indicated that the precipitation pattern is more symmetrical about the storm center when forward motion is slow, and concentrated in the front, especially the right front, when storm speeds are higher. A more important point of agreement between the various sets of data is that the greatest outward echo motion occurs to the left of the direction of eye motion. This is best shown by figure 29 which depicts radial and tangential echo speeds in knots for the 1569 echoes from seven storms studied in 1960 [7], and for the 3696 echoes from Donna.

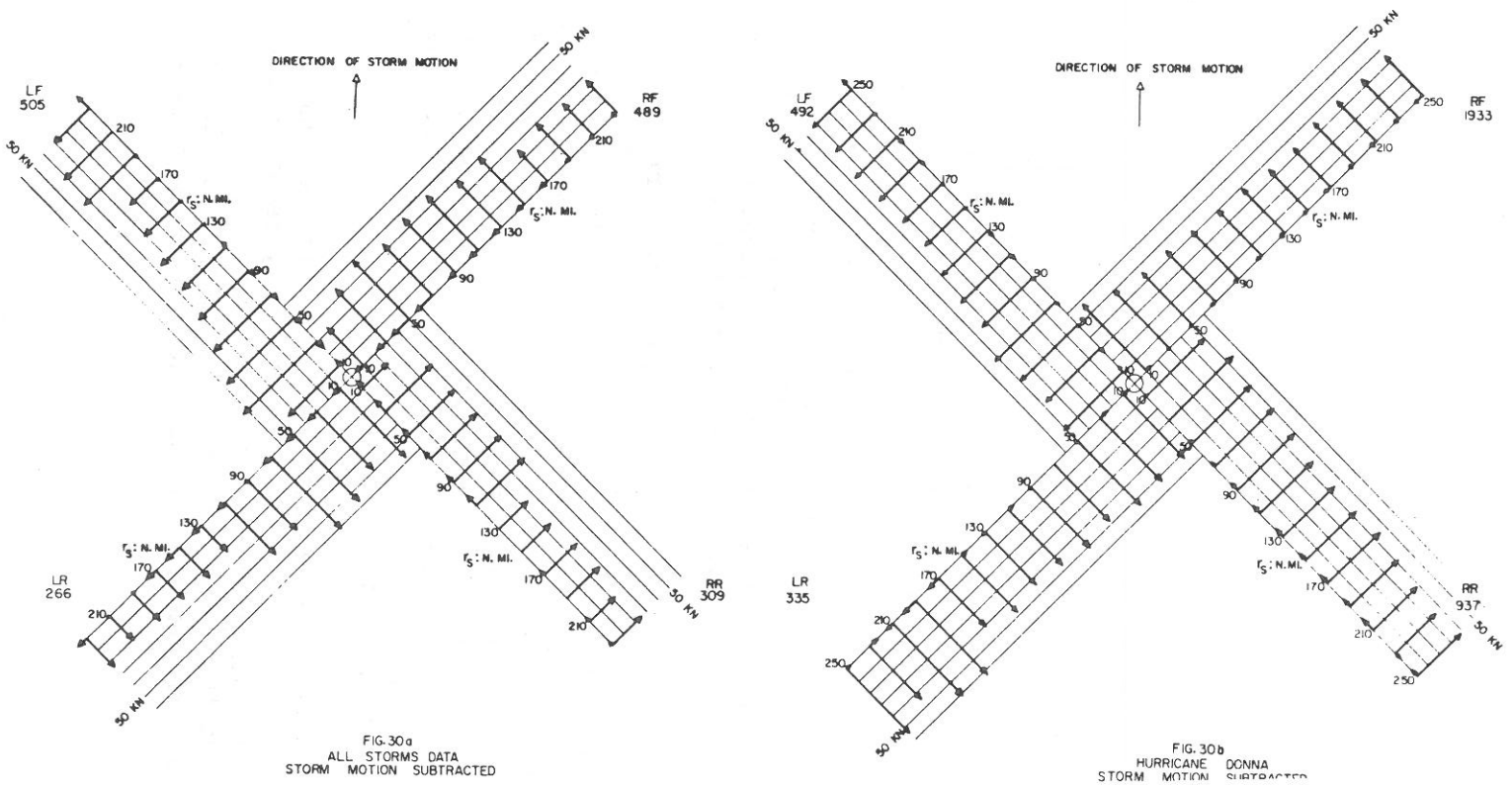

Figure 29. - Comparison of tangential and radial echo speeds for each quadrant of Donna and seven storms data: (a) All storm data, storm motion subtracted, (b) Hurricane Donna, storm motion subtracted.

Tangential echo speeds for the first 100 n. mi. from the storm center are highest in the left rear quadrant in both sets of data. Beyond that they drop off to relatively low levels, about 35-40 kt., in all quadrants except the left rear in Donna and the left front in data from the seven storms, where very significant increases are evident. In fact, the region containing the fastest individual small echoes (not "protuberances") in Donna, averaging over 60 kt., is beyond 180 n. mi. in the left quadrant.

When radial motion for the seven storms and Donna are compared in figure 29, it can be seen that general inward echo motion is indicated for both sets of data in the right quadrants. This is true except for the area nearest the eye in the right front, where outward motion is indicated in Donna. In the left front quadrant, data from the seven storms indicated essentially no radial motion. However, in the left front of Donna, inward motion exists equal to that in the Donna right front quadrant. Even the outward motion very near the eye in the right front of Donna is duplicated in the left front quadrant. The left rear quadrant has some inward motion near the eye, the strongest of any quadrant for those ranges; but at greater ranges outward echo motion is generally indicated, becoming strong at 170-210 n. mi. The data from the seven storms shows the strongest outward motion at slightly shorter ranges in the same quadrant.

It should be remembered that methods of arriving at storm motion, especially direction, influence the echo velocity and quadrant into which a given group of echoes is placed. It is considered very significant that the increase in speeds, the general speed profiles, and the gross features of outward radial motion appear in all three sets of data.

A special study of L_t for 67 echoes from hurricane Carla showed an average lifetime of exactly 35 min., the same as that for the Donna data. The card echoes were found at various ranges from the radar and at ranges out to 200 mi. from the storm center. The mean diameter of the echoes was 6.5 n. mi. For these data, d_e was plotted against L_t. As one might expect with radar echoes, some of which might be multi-celled despite attempts to be selective, the larger 7-8 mi. d_e echoes had lifetimes near 50 min. while the 4-5 mi. d_e echoes had lifetimes of only about 25 min. The Donna echo diameters were plotted against r_s and averaged about 6 n. mi. at 90 n. mi. range and 4.5 n. mi. at 180 n. mi. range.

Although range differences exist in both the echo diameter and lifetime of echoes found in the various sets of data, radar sampling bias severely limits the conclusions which might be drawn from them. The average lifetime of 35 min. and the average diameter of about 5 n. mi. for echoes is corroborated by all hurricane echo studies we have made to date.

4. FINE SCALE MOTION OF ECHOES

Although the above studies determined the general fields of large-scale echo motion in hurricanes, they were not adequate to describe the differences in echo motion which might exist in various smaller regions in and around spiral bands. For this purpose, a more selective study was begun on the hurricane Carla data using the plan shown in figure A4, Appendix. The results, although interesting, are based on a relatively small number of echoes from a Gulf Coast storm. They may not be directly compared to the previous "seven storms" or Donna data and must be considered preliminary in nature.

Since echoes vary in L_t, they were compared on the basis of their individual quarter lifetimes and separated into 50 mi. r_s, 30° θ_e, and environmental categories: I. those located inside spiral bands; II. those found outside of bands; and III. those in spiral band "tails", the upwind region of relatively distinct echoes, relatively far from the storm center, usually in the right rear quadrant.

When echo speed is studied considering the entire storm, it is found that echoes increase in speed from the first to second quarters of their lifetimes and decrease in speed from the second to third and last quarters. The decrease in speed from first to second half of echo L_t was evident at all ranges except the 150-200 n. mi. increment, where the maximum speed occurred during the third quarter.

When azimuth was considered, it was evident that speeds were greater in the left front quadrant for all quarter periods. Unexplained, however, is the observation that echoes directly ahead of the storm had speed maxima in the first quarter lifetime whereas, proceeding clockwise around the storm, the speed maxima occurred progressively later until the right rear quadrant maximum occurred in the third quarter. These echoes correspond largely to the 150-200 n. mi. r_s increment and are probably in spiral band "tails."

When spiral band environment was introduced as a parameter, the average speed was greater in spiral bands, least outside of the bands, and at intermediate values for the band tails.

Echo crossing angles were mostly negative in the 50-100 n. mi. r_s interval, most highly negative in the third (decreasing echo speed) quarter L_t. The largest percentage of positive crossing angles was found in the 200-250 n. mi. range. The echoes in the 150-200 n. mi. r_s increment (mostly in band tails) became progressively more positive in their L_t quarters.

Echoes located outside of bands had largest positive α_e in the second quarter, while those in band tails had the greatest negative α_e in that quarter, becoming less negative (or more positive) in the third and fourth quarters.

It is obvious that with so few echoes, some of the r_s or θ_e increments had no data, or were relatively unrepresentative of average conditions as a result of the extensive variations which exist in even the best echo motion data. These studies are being continued in an attempt to increase confidence in some of the above conclusions, as well as to answer important questions concerning the relative motion characteristics of echoes on opposite sides of the spiral bands. It is also desired to determine whether echoes tend to move across the spiral band or down-band as the band moves outward.

5. SUMMARY AND CONCLUSIONS

In the foregoing sections we have discussed the echo motion in several storms in general, and in one of these (the one for which we had the most data) the motion was discussed with considerably more precision and detail than had previously been attempted. By way of summary, we now list some of the important results, and discuss some of the conclusions which seem to be pertinent.

Consider first the location of echoes around the storm. After careful analysis we conclude that for most of these studies, echo altitude variations due to beamwidth and range bias do not noticeably influence the determination of echo velocities. In azimuth, we find nearly one-half of the echo sample in the right front quadrant, with very few echoes found in the left rear quadrant and the remainder of the echoes distributed evenly between the other two quadrants. In range, the largest group of echoes arrange themselves in a band between 70 and 110 n. mi. around the storm. The range distributions for low and medium storm speeds are more "normal" in that they peak higher and more sharply than the curve for high storm speed, which shows a considerable degree of disorganization in its three relatively low peaks.

If it can be assumed that radar location and other bias is unimportant, then it appears that this disorganization in the echo distribution at high storm speeds may be the result of some disturbance in the internal mechanism of the storm which is in some way connected to storm motion, thus giving rise to the sinusoidal storm speed fluctuations that are observed in the studies of small-scale eye motions [12].

Now consider the echo motions, which also give evidence of the presence of a propagating disturbance coupled to storm speed. In crossing angle, we find that most of the echoes in the right semicircle possess inward crossing angles; indeed, inward crossing angles predominate throughout the storm, except for a 100° segment directly to the left rear of the direction of storm motion. Inward moving echoes have larger absolute crossing angles than outward moving echoes. The fraction of echoes possessing inward crossing angles rises with the increasing storm speed, while the fraction of echoes possessing outward crossing angles falls. In speed, we find that outward moving echoes generally have higher speeds than inward moving echoes in the rear quadrants, the opposite being the case in the front quadrants. There is greater variation in echo speed with range from the storm center at high storm speed than at low storm speed, with the slowest echoes usually found in the right front quadrant and the fastest in the left rear quadrant. It is to be

particularly noted that echo speeds increase with increasing storm speed, while at the same time the absolute crossing angles decrease within 150 n. mi. For ranges greater than 150 n. mi. the reverse is the case. Completely unexpected is the fact that for the small echoes studied here the highest speeds are found to the left of the storm motion and in a region well away from the eye wall. Generally, echo speeds drop off gradually with range from the storm center but the profiles do not have either the relatively high speeds throughout the storm area or the pronounced speed maxima near the eye wall which characterize the surface wind field.

If echo and storm speed were coupled by a mechanism that originates near the center of the storm and propagates disturbances outward, then it would be expected that the echoes at extreme ranges and high storm speeds would not respond to the mechanism immediately, possibly not until the storm was moving slowly again.

It has been seen that the storm speed oscillations seem to be reflected in the echo motions with a delay factor which increases with range, as shown in figure 3. Since the period of the storm speed oscillation is of the order of 1/2 hour, the speed of its outward propagation to reach echoes 150 n. mi. away would have to be of the order of 300 kt. This suggests that the echo generating disturbances are not advected by the winds but might be propagating through the hurricane in the manner of pressure jump waves.

Attempts to gain echo motion information at various heights by stratifying the data according to range from the radar were inconclusive. However, the results of some of the horizontal echo motion studies, which show variations in both speed and crossing angle of echoes with storm speed and other parameters, can be used to infer a probabilistic picture of echo height if certain assumptions are made. To do this, one must temporarily ignore echo propagation effects and assume a roughly linear relationship between echo velocity and the mean wind vector for the levels in the atmosphere which affect the motion of the echo. Then echoes generated in the inflow layer (generally assumed to be at low levels) will be advected by those winds ($+\alpha_w$) resulting in $+\alpha_e$ until (and unless) they propagate into the outflow layer (generally assumed to be at high levels) where the vector sum of the winds acting on their total heights is sufficient to give outward motion ($-\alpha_w$), resulting in $-\alpha_e$. A rise in the fraction of echoes with $-\alpha_e$ would then indicate an increased proportion of echoes had reached higher levels; a decrease in the fraction of such echoes would indicate either a decrease in the number of echoes reaching higher levels or a relative increase in the number of echoes produced in, and remaining at lower levels. The data show that except in the left rear quadrant both echo velocity and the fraction of inward echo crossing angles rises with increasing storm speed. This would indicate that a decrease in the levels at which most echoes are found occurred with an increase in storm speed in Donna. It is well known that relations also exist between convective activity and echo heights, which may in turn be related to echo motion and storm motion by the above analysis; but available data are not yet sufficient to study and document such relationships.

It was seen in section 3 that inward moving echoes in the front quadrant had higher speeds than outward moving echoes and that the situation generally reversed in the rear of the storm, especially the left rear. This effect can only be explained by an inward component in the two forward quadrants and an outward component in the two rear quadrants. If the echo directions are taken as representative of winds and a large number of echoes is considered somewhat indicative of convergence, then echo convergence is indicated for the right front quadrant and divergence for the left rear quadrant. The possible ventilation effects indicated would also tend to make echoes in both right quadrants move a bit more slowly than those in the left quadrants, an observation which agrees well with our earlier results of echo motion in all storms.

Quantitative conclusions with regard to echo height as a function of crossing angle are, however, very difficult to make, since a cloud tower has a high degree of lateral inertia imparted to it by its low-level convective generation. An echo with its base in the inflow layer does not react to the stresses imparted to it by the wind field until its top is at the level of the outflow layer, say 5 or 6 n. mi. high. Much of the tower is then in the outflow layer, and the stresses combine to give its resultant motion outward crossing angle, thus leading perhaps to the breaking away of the echo tower from its base, and the resulting disintegration of the cloud itself. During such a process significant amounts of water may be raised to the middle and higher levels, to remain as multi-cloud layers generally moving with the winds associated with those layers.

Considerable differences exist in the motions of echoes found over water and those over land, as well as between those studied during day and night periods. Although some radar position bias is admittedly present for the former, both of the transitions indicate that the echoes become more concentrated near the core region when the storm is over land, and at night. The effect of the different atmospheric conditions prevailing at night causes the storm to become more compact and symmetrical and more closely organized in the core region. The night storm is also generally less intense than the day storm and has somewhat lower wind speeds, if the echoes are used as indicators. The night echoes were found to move slightly slower than the day, and the land echoes to move faster than the over-water echoes. The echo data should also lead to the conclusion that the storm becomes smaller and more concentrated as it moves from the water to the land environment. As a matter of fact, Donna did not maintain its over-water state (intensity, maximum winds, lowest pressure, etc.), but lost considerable intensity as it moved across the Florida peninsula, as most storms do after making land-fall. However, the radar bias mentioned above forbids any strong conclusions to be made directly from the data.

When echo-wind relationships are studied using relatively concurrent land-based radar data and NHRP flight data, it appears that there are significant differences between the relationships from quadrant to quadrant. Echoes in the right front quadrant move more slowly than winds at low and middle levels but with crossing angles nearest the winds at 14,000 ft.; echoes in the right rear quadrant have greater inward crossing angles than all the winds plotted, but their speeds are near the wind speeds; the echoes

in the left quadrants more nearly approximate the wind speeds and directions at the 1,600- and 1,400-ft. levels. It has been felt for some time that echo-wind relationships are severely complicated by propagation components, and the present studies tend to confirm this theory.

It seems apparent from the above that when echo motion is compared to winds at the various levels reported here for Donna, it cannot be said that the echoes follow the winds at a particular level in all regions of the hurricane. Instead, it appears from the very limited observations to date that there are significant differences in the echo-wind relationships in the right quadrants. Until far more data become available, one can only hypothesize that echoes in the right quadrants (especially the right front) move more slowly than the winds because they are in a low-level region of generation and are being "ventilated." In the left quadrants (especially the left rear), the echoes may be in the dissipating stages at somewhat higher levels and subject to more simple wind transport without affecting their immediate environment as much as those in the right quadrants.

Although their data did not pertain to hurricanes and was rather limited at higher speeds, the Thunderstorm Project [2] found that "radar-cloud" movement was considerably slower than the mean wind speed in the gradient to 20,000-ft. layer when winds exceeded 20 m.p.h. Since almost all of our echoes are found in regions of higher wind speeds, we should not expect the precipitation elements to exactly follow the local winds. The important question which remains is why they appear to follow the winds in some regions very closely and not in others.

The statement was made intuitively several years ago [11] that spiral bands get their shape from disturbances in the low-level flow, but that their echo components move generally in accordance with the flow at higher levels. This is now at least partially confirmed by the results of these studies. Our observation of negative α_e for echoes in bands means that if such echoes are to "seed" additional echoes downwind, as proposed by Atlas [1] the spiral band must be moving outward. This is also the case even for the spiral band "tails", which Atlas called a region of "generators", where α_e and α_w (wind crossing angles) are near zero but where α_b (band crossing angle) is maximum inward. Further work needs to be done on this problem, but it presently appears impossible for echoes to generate other echoes downwind, except with a large component normal to the band and possibly near the wall cloud (a region not discussed by Atlas), because the bands generally do not appear to move outward as fast as the observed v_e component normal to the band.

All of the above data shows that there are generally large differences between echoes in the various quadrants of the hurricane; and some of the differences become even more apparent when the data are divided into 30° segments of θ_e. Then it appears that the logical and most convenient dividing line through the hurricane from the point of view of echo generation and motion is from the center of the right rear quadrant through the center of the left front quadrant.

Echo motion studies are continuing, but on a finer scale than previously. The differences in the small-scale motion of echoes inside and outside of bands and the analysis of that motion with regard to the local winds and storm speed deserve further effort.

The differences between echo motion and wind, all of which we include under the term "propagation effects", remain as one of the most important studies to be made when data finally become available on echo motion concurrent with relatively local multi-level winds in the echo environment. A separation of propagative and advective components, if possible, would lead to significant advances in understanding the echoes and convective processes as well as the role of spiral rain bands in hurricanes.

6. ACKNOWLEDGMENTS

These studies would not have been possible without the excellent cooperation and assistance afforded by the National Hurricane Research Project as well as other personnel from the Weather Bureau, the U. S. Navy, and the U. S. Air Force who helped to gather and supply much of the data necessary to the project. Credit is also due to Professor Homer W. Hiser, Head of the Radar Meteorological Section, who helped gather some of the data, and to other Radar Laboratory personnel who maintained and operated the radar equipment. Finally some of the painstaking data reduction was done by student assistants partly supported by National Science Foundation Undergraduate Research Participation Grants.

REFERENCES

1. D. Atlas, K. R. Hardy, R. Wexler, and R. J. Boucher, "On the Origin of Hurricane Spiral Bands," Geofisica Internacional, vol. 3, No. 3-4, 1963, pp. 123-132.

2. H. R. Byers, et al., The Thunderstorm, U. S. Weather Bureau, Washington, D. C., 1949, 112 pp.

3. L. F. Conover, "Evaluation of Eye Fixes Obtained by Radar for Hurricane Donna September 1960," Proceedings, Second Technical Conference on Hurricanes, American Meteorological Society, Miami Beach, Florida, June 1961, pp. 85-100.

4. M. G. H. Ligda, and W. A. Mayhew, "On the Relationship Between the Velocities of Small Precipitation Areas and Geostrophic Winds," Journal of Meteorology, vol. 11, No. 5, Oct. 1954, pp. 421-423.

5. V. A. Myers, and W. Malkin, "Why is the Hurricane Wind Field Asymmetrical," U. S. Weather Bureau, Washington, D. C. 1959. (unpublished)

6. H. V. Senn, and H. W. Hiser, "Effectiveness of Various Radars in Tracking Hurricanes," Proceedings, Second Technical Conference on Hurricanes, American Meteorological Society, Miami Beach, Florida, June 1961, pp. 101-114.

7. H. V. Senn, and H. W. Hiser, "The Mean Motion of Radar Echoes in the Complete Hurricane," Proceedings, Eighth Weather Radar Conference, American Meteorological Society, San Francisco, California, April 1960, pp. 427-434.

8. H. V. Senn, and H. W. Hiser, "The Origin and Behavior of Hurricane Spiral Bands as Observed on Radar," Proceedings, First Technical Conference on Hurricanes, American Meteorological Society, Miami Beach, Florida, Nov. 1958, p. C-13.

9. H. V. Senn, and H. W. Hiser, "Studies of the Evolution of Hurricane Spiral Bands and Their Relationship to Other Synoptic Storm Parameters 1 July 1957 to 30 June 1958," Final Report, 8899-1, (ASTIA AD-205540) on Contract Cwb-9174, Aug. 1958.

10. H. V. Senn, H. W. Hiser, and E. F. Low, "Studies of the Evolution and Motion of Hurricane Spiral Bands and the Radar Echoes Which Form Them 1 July 1958 to 30 June 1959," Final Report, 8924-1, (ASTIA AD-227258) on Contract Cwb-9480, Aug. 1959.

11. H. V. Senn, H. W. Hiser, and R. C. Bourret, "Studies of Hurricane Spiral Bands as Observed on Radar 1 October 1955 to 1 December 1956," Final Report, 57-1, (ASTIA AD-271061) on Contract Cwb-9066, Jan. 1957.

12. H. V. Senn, H. W. Hiser, and J. A. Stevens, "Radar Hurricane Research 1 July 1961 to 30 June 1962," Final Report, 8982, (ASTIA AD-291185) on Contract Cwb-10198, University of Miami, Institute of Marine Science, Coral Gables, Florida, Sept. 1962, 109 pp.

13. H. V. Senn, H. W. Hiser, J. A. Stevens, and E. F. Low, "Radar Hurricane Research 1 July 1960 to 30 June 1961," Final Report, 8858, (ASTIA AD-264959) on Contract Cwb-9940, University of Miami, Institute of Marine Science, Coral Gables, Florida, Aug. 1961, 96 pp.

APPENDIX - I.B.M. CARD FORMATS

DONNA #1	DONNA #2*	DONNA #3**	DONNA #1***	COL
- Storm #	] Blank	] Blank	- Storm #, (1)	1
] Month	] 73-74	] 3-4	] Month, (1)	2 3
] Day	- Blank	] Blank	] Day, (1)	4 5
] Year	] 76-77	] 7-8	] Year, (1)	6 7
] Begin E.S.T.	] Blank	- Blank	] Begin E.S.T., (1)	8 9 10
- L_t(C)	] 24-26	] D_o(c)	- L_t, (1)	11 12
] Radar I.D.(C)	] Blank	] Blank	] Radar I.D., (1)	13 14
]	] 27-28	] v_o(c)	]	15 16
]	- Blank	- Blank	] Blank	17
] Blank	] 29-31	] θ_e(c)	] D_o, (3)	18 19
]	- Blank	- Blank	] v_o, (3)	20 21
]	] 32-34	] r_s(c)	- Blank	22 23
] D_{s2}(mC)	- Blank	- Blank	] D_{s2}, (1)	24 25
] v_{s2}(mC)	] 35-37	] D_e(c)	] v_{s2}, (1)	26 27
] θ_e(m)	] Blank	- Blank	] θ_e, (3)	28 29 30
]	] 42-43	] v_e(cC)		31
] r_r(M)	- Blank	- Blank	] r_r, (1)	32 33
]	- 47	] α_e(cC)	] r_s, (3)	34 35 36
] r_s(m)	] 45-46	] Blank	- Blank	37 38
]	] Blank	] v_r(c)	] D_e, (3)	39 40
] Blank	- 55	] Blank	] v_e, (3)	41 42
]	] Blank	] v_θ(c)	- Blank	43 44
] v_e(m)	- 56	] Blank	] α_{e2}, (3)	45 46
- Blank	] Blank	] k_1(cC)	- Sign α_e,v_r,k_1, (3)	47
] α_e(m)	] 58-59	- Blank	- Blank	48
- 11 if α_e Neg.	- Blank	- Sign on k_2(C)	] v_r, (3)	49 50
]	] 62-64	] k_2(cC)	- Blank	51
] Blank	] Blank	] Blank	] v_θ, (3)	52 53
]			- Blank	54
]			- Tracing Basis, (1)	55
- Tracing Basis (C)	] 65-66	] 59-60	- Time Basis D_{s2},v_{s2},(1)	56
- Time Basis D_{s2},v_{s2}(C)			- Blank	57
- Blank	] Blank	] Blank	] R, (1)	58
] R	] 4-5	] 15-16	] k_1, (3)	59 60
] Blank				61
]			] D_{s1}, (1)	62 63
] D_{s1}(MC)				64
] v_{s1}(MC)			] v_{s1}, (1)	65 66
]			- Sign on α_{e1}, (1)	67
] Blank			] α_{e1}, (1)	68 69
]	] Blank	] Blank	- Sign on k_2, (3)	70
]			] k_2, (3)	71 72
] Tracing #			] Tracing #, (1)	73 74
] Blank			- Blank	75
] Echo #			] Echo #, (1)	76 77
]				78
] Blank			] Blank	79 80

(C) Coded - See explanation next page.
(c) Computed or recomputed value - See Fig. 9, sect. 4 and text for definition.
(M) Measured value from tracing.
(m) Measured value but not from tracing; or measured from tracing but later replaced by a computed correct value.
* Data from indicated cols. in Donna #1. Input to Donna I program, see text.
** Answers to Donna I program. Cols. indicate data from Donna #2. Input to program Donna II, III, and IV, see text.
*** Master deck combining corrected data of deck #1 (1) with computed data of deck #3 (3).

Figure A1. - Hurricane Donna echo deck

COL	7 STORM DATA
1	- Storm #
2 3	] Month
4 5	] Day
6 7	] Year
8 9 10 11	] Begin E.S.T.
12	- Time L. (C)
13 14	] Radar I.D.(C)
15 16 17	] Blank
18 19 20	] D_o(M)
21 22	] v_o(M)
23	- Blank
24 25 26	] D_s(m)
27 28	] v_s(m)
29	- Blank
30	- Echo Quad (C)
31	- Blank
32 33 34	] r_r (M)
35 36 37	] r_s(M)
38	- Blank
39 40 41	] D_e(M)
42 43	] v_e(M)
44	- Blank
45 46	] α_e(M)
47	- 11 if α_e Neg.
48	- Blank
49 50	] v_r(c)
51	- Blank
52 53	] v_θ(c)
54 55 56 57	] Blank
58 59	] R
60 61 62 63 64 65 66 67 68 69 70 71 72 73 74 75	] Blank
76 77 78	] Echo #
79 80	] Blank

Figure A2. - Seven storms echo deck

COL.

12 Time Length of Echo Traced-Punch 1: under 15 min; 2: 15-30 min; 3: 31-60 min; 4: over 60 min.

13-14 Radar I.D. and Location

Punch		Punch		Punch	
01. Boca Chica	SX	11. Chas. W.B.	WSR-1	21.	
02. Cape Chas.	FPS-3	12. Nantucket	SP	22. Eglin	CPS-9
03. Cape Hat.	SP	13. Univ. Miami	SP-1M	23. AQQC	WSR-57
04. San Juan	SP	14. Patrick	CPS-9	24. DAB	WSR-57
05. F.W.C. Miami	CPS-9	15. Univ. Miami	MPS-4	25. NIP	CPS-9
06. S. Truro	FPS-3	16. MIAC	WSR-57	26. MacDill	CPS-9
07. Cape Chas.	FPS-4	17. EYW	WSR-57	27. MacDill	FPS-20
08. M.I.T.		18. Key West	FPS-37	28.	
09. Ellington	CPS-6B	19. Key West	FPS-6	29.	
10. Alexandria	ADC	20.		30. Tampa	WSR-57

24-26 D_s blank for zero v_s or missing data.

27-28 v_s blank for missing data, punched zeros for zero storm speed.

30 Echo Quadrant-Punch 1: right front; 2: right rear; 3: left rear; 4: left front.

58-59 R blank if missing, punched zeros for zero eye radius. Donna II supplied 08 (mean) for 400 + missing R's.

DONNA #1 - 3805 CARDS

12 Time Length of Echo Tracing in # of 5 min periods (not necessarily entire lifetime of echo).

13-14 Radar I.D. and Location: same as 7 Storms Data.

24-26,62-64 D_{s1} and D_{s2} same as 7 Storms Data.

27-28,65-66 v_{s1} and v_{s2} same as 7 Storms Data.

55 Tracking Basis-Punch 1: Storm center held fixed while tracing echo; 2: Radar center held fixed while tracing echo.

56 Time Length Basis of v_{s2}-Punch 1: hourly mean storm speed used; blank if 30 min mean storm speed used.

DONNA #2 - 3805 CARDS

This deck has same items as Donna #1 transferred positionally for computational convenience only.

DONNA #3 - 3696 CARDS

30-32 v_e(c)can exceed 100 while v_e(m) Donna #1 could not.

34-36 α_e Col 36 and/or 35 are signif. digits; Col 34 or 35 sign α_e: 11 if neg., blank if zero or pos.

50 sign on k_2: punch 1 if negative, 2 if zero or positive.

47-48,51-52 k_1, k_2 left col. signif. digit, right col. power of 10 nec. to approx. k_1, k_2.

DONNA #1A - 3805 CARDS

47,67,70 Sign on α_e, k_1, k_2 indicated by blank if positive, 11 punch if negative.

Additional Notes for 7 Storms Data and Donna #1

1. If data group is more than 1 col. wide but data is only one number, punch zero in left spaces: Month 9 = 09; storm direction $2^\circ = 002^\circ$, etc.
2. If any data is missing, punch NO card for that echo. (Donna I substitutes R=8 if R blank).
3. Punch "X" (or 11) col. 47 if α_e is negative. Leave BLANK if positive.
4. No crossing angles greater than 90°.
5. Col. 18-22 is blank where tracing made holding storm center constant on Donna #1 only.
6. If v_o, v_e, v_θ greater than 100, punch 99. About 6 such cards were sorted out and deleted computations on Donna programs.
7. v_r, k_1 and α_e all take sign from col. 47: Blank if positive, 11 punch if negative.

Figure A3. - Codes and explanations of A1 and A2

1 - Storm # C
2, 3] Mo
4, 5] Day
6, 7] Year
8, 9, 10, 11] Begin ____ Time
12 - L_{te} *
13, 14] Radar I.D. C C
15, 16] α_b or 1
17 - Sign on α_b or 1
18, 19, 20] D_{oe} *
21, 22] V_{oe} *
23 -
24, 25, 26] D_{s2}] FROM INDEP. PLOT MEAN W.
27, 28] V_{s2}
29, 30, 31] θ_e *
32, 33, 34] r_{re} *
35, 36, 37] r_{se} *
38 - Echo Environ. C
39, 40, 41] D_e *
42, 43] V_e *
44 - d_e, Echo Diam. Mi.
45, 46] α_{e2}
47 - Sign α_{e2}, v_r, k_1 C
48 - Echo Type. C
49, 50] v_{re} *
51 -
52, 53] $v_{\theta e}$ *
54 -
55 - Trac. Basis C
56 - Time Basis D_{s2}, V_{s2} C
57 -
58, 59] R, Eye Radius
60, 61] k_1 C
62, 63, 64] D_{s1}] FROM TRAC.
65, 66] V_{s1}
67 - Sign α_{e1} C
68, 69] α_{e1}
70 - Sign k_2 C
71, 72] k_2 C
73, 74] Trac. #
75 - d_b or 1 Sp.B.Width C
76, 77] Echo #
78, 79] ω_b (Radians,Tenths)/Hr
80 - Sp. Band Data C

DITTO DATA SHEET INSTRUCTIONS AND CODES HVS 12/62

*If Col. 80 punched, these Subscr. may change to b or 1

OBSERVER DATE

INSTRUCTIONS

1. Before making study, care. check off cols. which will not be used: fill in all others.
2. Use every other line of data sheet, # trac. from 99 backwards consecutively for each radar.
3. If data missing leave blank, not zeros.
4. If data group more than 1 col. wide but data only one #, punch 0 in left spaces: Mo 9 = 09: D_s 2^o = 002^o, etc.
5. No provision for crossing angles greater than 90^o.
6. If v_o, v_e, v_θ, etc. greater than 100, enter true speed, Code 99.
7. Sign v_r, k_1 and α_e in col. 47.
8. Subscripts: s-from, or of, storm center
   e-echo
   b-spiral band

Col CODES FOR C

1: Storm #1 = A, 2 = B etc., each year.
12: L_t, # 5-min intervals: 1-10; over, Code 11.
13-14: Radar I.D. (See Code).
38: Echo Environ: 1, in Sp.B.; 2, in Sp.B.tail; 3, in Pre-H. Sq. L.; 4, in rain sh.; 5, outside Sp.B., rain sh., or " "
47, 67, 70: Signs: Blank, enter - (11 punch) neg.
48: Echo type-1: indiv. round echo; 2: multi-cell echo; 6: protub. elsewhere; 7: protub. within band; 8: protub. on inside edge of band; 9: protub. on outside edge band.
55: Track. Basis 1: St.C. fixed on trac.; 2: radar C. fixed.
60-61, 71-72: k_1, k_2: l. col. signif. dig., r. col. power 10
75: d_b Sp.B.W.: Enter 1/2 true W. (11 if over 20).
80: Sp.B. Data: Bl, Reg echo data, some Sp.B. data; 1: Sp.B. (b) only; 2: Pre-H. Sq. L. (l) only.
56: Time Basis: 1, Hr. Mean V_s, D_s; 2, 30 Min. V_s, D_s.

Figure A4. - Hurricane Carla echo data format

TR 3170-74
Senn...
A SUMMARY OF EMPIRICAL STUDIES OF THE HORIZONTAL MOTION OF SMALL RADAR PRECIPITATION ECHOES IN HURRICANE DONNA AND OTHER ...

TR 3170-74
Senn...
A SUMMARY OF EMPIRICAL STUDIES OF THE HORIZONTAL MOTION OF SMALL RADAR PRECIPITATION ECHOES IN HURRICANE DONNA AND OTHER...

(Continued from inside front cover)

No. 46. Some aspects of hurricane Daisy, 1958. H. Riehl, J. Malkus. July 1961.
No. 47. Concerning the mechanics and thermodynamics of the inflow layer of the mature hurricane. S. L. Rosenthal. September 1961.
No. 48. On the structure of hurricane Daisy (1958). José A. Colón and Staff. October 1961.
No. 49. Some properties of hurricane wind fields as deduced from trajectories. Vance A. Myers and William Malkin. November 1961.
No. 50. Proceedings of the Second Technical Conference on Hurricanes, June 27-30, 1961, Miami Beach, Fla. M. A. Alaka. March 1962.
No. 51. Concerning the general vertically averaged hydrodynamic equations with respect to basic storm surge equations. Heinz G. Fortak. April 1962.
No. 52. Inventory, use, and availability of NHRP meteorological data gathered by aircraft. H. F. Hawkins, F. E. Christensen, S. C. Pearce and Staff. April 1962.
No. 53. On the momentum and energy balance of hurricane Helene (1958). B. I. Miller. April 1962.
No. 54. On the balance of forces and radial accelerations in hurricanes. W. M. Gray. July 1962.
No. 55. Vertical wind profiles in hurricanes. H. T. Hawkins. June 1962.
No. 56. A theoretical analysis of the field of motion in the hurricane boundary layer. Stanley L. Rosenthal. June 1962.
No. 57. On the dynamics of disturbed circulation in the lower mesosphere. R. H. Simpson. August 1962.
No. 58. Mean sounding data over the western tropical Pacific Ocean during the typhoon season. and Distribution of turbulence and icing in the tropical cyclone. Kenji Shimada and Z. Hashiba. October 1962.
No. 59. Reconstruction of the surface pressure and wind fields of hurricane Helene. Charles E. Schauss. October 1962.
No. 60. A cloud seeding experiment in hurricane Esther, 1961. R. H. Simpson, M. R. Ahrens, and R. D. Decker. November 1962.
No. 61. Studies on statistical prediction of typhoons. H. Arakawa. April 1963.
No. 62. The distribution of liquid water in hurricanes. B. Ackerman. June 1963.
No. 63. Some relations between wind and thermal structure of steady state hurricanes. Herbert Riehl. June 1963.
No. 64. Instability aspects of hurricane genesis. M. A. Alaka. June 1963.
No. 65. On the evolution of the wind field during the life cycle of tropical cyclones. José A. Colón. November 1963.
No. 66. On the filling of tropical cyclones over land, with particular reference to hurricane Donna of 1960. B. I. Miller. December 1963.
No. 67. On the thermal structure of developing tropical cyclones. Edward J. Zipser, Jr. January 1964.
No. 68. Criteria for a standard project northeaster for New England north of Cape Cod. K. R. Peterson, H. V. Goodyear, and Staff. March 1964.
No. 69. A study of hurricane rainbands. R. C. Gentry. March 1964.
No. 70. Some theoretical results which pertain to the upper-tropospheric vortex trains of the Tropics. S. L. Rosenthal. April 1964.
No. 71. Energy generation and flux processes associated with a weakening depression over the Gulf of Mexico. M. A. Lateef. June 1964.
No. 72. On the structure of hurricane Helene (1958). J. A. Colón. December 1964.
No. 73. On the scales of motion and internal stress characteristics of the hurricane. William M. Gray. October 1965.